Global and Planetary Change 259 (2026) 105315

Contents lists available at ScienceDirect

Global and Planetary Change

journal homepage: www.elsevier.com/locate/gloplacha

Review Article

Holocene relative sea-level changes from the Atlantic coasts of South America

K. Rubio-Sandoval [a,b], T.A. Shaw [c], M. Vacchi [d], N. Khan [e], B.P. Horton [f], J.R. Angulo [g], M. Pappalardo [d], A.L. Ferreira-Júnior [h], S. Richiano [i], M.C. de Souza [g], P.C. Giannini [j], D.D. Ryan [d], E.J. Gowan [k,l], A. Rovere [a,m,*]

[a] MARUM - Center for Marine Environmental Sciences, University of Bremen, Bremen, Germany
[b] Instituto de Geociencias, Universidad Nacional Autónoma de México, Querétaro, Mexico
[c] Earth Observatory of Singapore, Nanyang Technological University, Singapore, Singapore
[d] Department of Earth Sciences, University of Pisa, Italy
[e] Departament of Earth Sciences, University of Hong Kong, Hong Kong, China
[f] School of Energy and the Environment, City university of Hong Kong, Hong Kong, China
[g] Departamento de Geologia, Universidade Federal do Paraná, Paraná, (UFPR), Brazil
[h] Pós-graduação de Genética Evolutiva e Biologia Molecular, Universidade Federal de São Carlos (UFSCar), São Paulo, Brazil
[i] Patagonian Institute of Geology and Paleontology, IPGP-CENPAT-CONICET, Argentina
[j] Departamento de Geologia, Universidade do São Paulo (USP), Brazil
[k] Department of Earth and Environmental Sciences, Kumamoto University, Kumamoto, Japan
[l] KIKAI institute for Coral Reef Sciences, Kikaijima, Japan
[m] Department of Environmental Sciences, Informatics and Statistics, Ca' Foscari University of Venice, Venice, Italy

ARTICLE INFO

Editor name: Dr. Fabienne Marret-Davies

Keywords:
Holocene database
Argentina Holocene Sea level
Uruguay Holocene Sea level
Brazil Holocene Sea level
Past sea-level changes Atlantic coast of South America

ABSTRACT

Holocene relative sea-level (RSL) changes along the Atlantic coast of South America reflect a complex interplay between ice equivalent sea-level, glacio-isostatic adjustment (GIA), regional tectonics, and local sedimentary processes. However, the uneven spatial and temporal resolution of existing Holocene RSL data has hindered regional assessments. Here, we compile and standardize 1108 RSL data points from Brazil, Uruguay, Argentina, and Chilean Tierra del Fuego, creating the first comprehensive database for the southwestern Atlantic. The data reveals a widespread Mid-Holocene highstand between 7000 and 4000 years BP, with RSL rising 2 to 4 m above present-day sea level, followed by a gradual fall to present. This pattern is consistent with GIA model predictions across the region's $> 50^{\circ}$ latitudinal span. Peak rates of RSL change occurred during the Early to Mid-Holocene transition, reaching up to 17.2 mm/yr in Tierra del Fuego and decreasing to 1.6 mm/yr near the Amazon delta. After 5000 years cal BP, RSL started to fall at 0.5 mm/yr. This Atlantic coast of South America database fills a critical geographic gap and provides a robust framework for refining GIA models and understanding sea-level evolution during the Holocene in the Southern Hemisphere.

1. Introduction

The study of Holocene RSL changes is fundamental to understanding how sea level responds to ice melting, the subsequent glacial isostatic adjustment (GIA) signal (e.g., Milne and Mitrovica, 2008; Björck et al., 2021), as well as other vertical land motions caused tectonics or sediment compaction (e.g., Rabassa et al., 2000; Khan et al., 2015; Garrett et al., 2020). Most studies of Holocene RSL change are local in nature, as they report the age and elevation of sea level index points (SLIPs) at specific locations. However, there is a long-lasting effort in the sea-level community to standardize SLIPs into sea-level databases with wider regional to global coverage (Tushingham and Peltier, 1992; Düsterhus et al., 2016; Khan et al., 2019; Rovere et al., 2023).

A renewed coordinated effort to build a global Holocene sea-level database was undertaken by the HOLSEA project (Khan et al., 2019), which promoted the use of rigorous standards for the reporting of sea-level data initiated in the late 80's and early 90's (van de Plassche, 1986; Pirazzoli, 1991; Shennan et al., 1993; Shennan, 2015). The

* Corresponding author at: Ca' Foscari University of Venice, Italy
E-mail address: alessio.rovere@unive.it (A. Rovere).

https://doi.org/10.1016/j.gloplacha.2026.105315
Received 31 July 2025; Received in revised form 21 December 2025; Accepted 14 January 2026
Available online 16 January 2026

advantage of such standardization resides in the possibility to investigate spatial and temporal trends of RSL changes, enabling comparison with GIA models and, ultimately, to improve our knowledge on the timing and modes of ice sheet melting since the Last Glacial Maximum (LGM), in turn helping inform future sea-level rise scenarios (Horton et al., 2018). In the context of this new effort to standardize Holocene sea-level data globally, there is a notable spatial gap: the Atlantic coasts of South America, in the southwestern Atlantic.

Holocene RSL along the Atlantic coasts of South America is not a knowledge gap, as the study dates back to the 19th century. One of the earliest documented observations comes from Darwin (1851), who described shoreline deposits above present-day sea level along the Argentine coast. Shortly thereafter, in the Brazilian coastlines, Hartt (1870) identified sea urchin beds above the high tide level (HTL) in Rio de Janeiro and interpreted the urchin beds as indicators of past higher sea levels. At the end of the 19th and beginning of the 20th centuries, John C. Branner drew initial paleo sea-level inferences for the Fernando de Noronha archipelago and the northeast Brazilian coast (Branner, 1889, 1890, 1902, and 1904). Backeuser (1918) used rock-boring mollusks to estimate sea-level changes along the coastline between Rio de Janeiro and Santa Catarina. van Andel and Laborel (1964) published the first radiocarbon dates, enabling not only more reliable spatiotemporal paleo-sea-level reconstructions but also the quantification of the timing of sea-level changes. In the 1980s, Porter et al. (1984) quantified Holocene RSL changes in Tierra del Fuego, Argentina, and Chile; and a decade later, the Holocene RSL variations in Uruguay began to be analyzed with the work of Bracco (1991), and Bracco and Ures (1998). Since then, sea level research in the southwestern Atlantic has evolved with several studies investigating more areas and progressively better age control. More recent work investigated Holocene RSL variations due to GIA (e.g., Rostami et al., 2000; Milne et al., 2005).

Four seminal research papers summarizing Holocene RSL changes in the region provide data with some degree of standardization and formed the starting point of our review. Frist, Angulo et al. (2006) compiled sea-level data along the Brazilian coastlines. They report and discuss the implications of more than 35 years of research by different groups and focus on RSL variations in the Mid to Late Holocene. While highlighting discrepancies in the reported data, they describe a common trend of a Mid-Holocene highstand with a subsequent fall to present-day sea level. Second, Bracco et al. (2011) describe the origin and geomorphological history of the Castillos Lagoon deposits, Uruguay, whose elevations decrease from ~4 m to ~2 m from the Mid to Late Holocene. However, they also describe SLIPs at elevations lower than 1 m around 4500 years cal BP. Third, Martínez and Rojas (2013) draw a RSL curve based on data from beach ridge deposits, showing that the Uruguayan sea level was above the present-day level at approximately 6000 years cal BP and has been declining since then. Finally, Schellmann and Radtke (2010) offer a wide review of SLIPs surveyed along the middle and south Patagonian Atlantic coast. According to the authors, beach ridges and valley mouth terraces data show varying elevations throughout the Holocene. They estimate the Holocene sea-level transgression peaked at 6900 years cal BP, with RSL about 2–3 m, and lasted until at least 6200 years cal BP, after which sea level declined to its present-day level. They also suggest that the mid and south Patagonian coast has likely been undergoing a slow glacio-isostatic uplift on the order of 0.3–0.4 mm/yr since Mid-Holocene. Some of this uplift resulted from the deglaciation of the Patagonian ice sheet, which covered the Andes Mountains in Chile and Argentina. Though the volume of the Patagonian ice sheet was relatively small (< 1.5 m sea level equivalent at the LGM, Davies et al., 2020; Gowan et al., 2021b), it may impact the RSL history in southern South America (Björck et al., 2021).

Here, we review published literature data to make a new, standardized regional Holocene sea-level database for the Atlantic coasts of South America. For all data, we standardized elevation measurement errors, indicative meanings, and recalibrated radiocarbon ages following HOLSEA protocol (Khan et al., 2019), ensuring consistency and comparability with other datasets globally. Through this framework, we aim to investigate spatio-temporal patterns of Holocene RSL, improve our understanding of the RSL trends driven by postglacial ice melting, thereby strengthening the foundations for future sea-level projections.

2. Regional setting

The Holocene sea-level database for the Atlantic coasts of South America spans the southwestern Atlantic from the coasts of Brazil, Uruguay, Argentina, to the Chilean part of Tierra del Fuego (Fig. 1A). The region of interest is located on the South America Plate and is, for the most part, a passive margin (Fig. 1A). However, toward the northern part of Brazil (e.g., Pernambuco and Paraiba), several authors have documented an increase in seismicity and highlighted the presence of faults offsetting Neogene deposits (i.e., Barreto et al., 2002; Bezerra and Vita-Finzi, 2000). In the far south, Tierra del Fuego is affected by the interaction between the Antarctic, Scotia, and South American plates (Isla and Angulo, 2016). Therefore, tectonics may play a role in the displacement of sea-level data in these two areas (Fig. 1: regions 3 and 12).

The area covered by the database encompasses a variety of coastal environments along the southwestern Atlantic margin. These include estuaries, coastal lagoons, deltas, sandy beaches, and rocky shorelines, each with distinct sedimentary processes that influence the formation and preservation of sea-level indicators (Dominguez et al., 1990; Codignotto et al., 1992; Behling et al., 2004; Schellmann, 2007). In addition to this geomorphological variability, tidal regimes also differ across the region. Along the Brazilian coast, tidal ranges span from microtidal conditions in the south to macrotidal in the northern regions, particularly in regions such as the Amazon River area (Melo et al., 2016). The Uruguayan coast is predominantly microtidal, with tidal amplitudes typically below 1 m (Martínez and Rojas, 2013). In contrast, much of the Argentine coast is mesotidal, with average tidal ranges around 1.7–2 m in open coast settings such as Mar del Plata (Santamaria-Aguilar et al., 2017).

3. Methods

The Holocene sea-level database for the Atlantic coasts of South America was compiled following the standardized protocol developed by the HOLSEA project (Khan et al., 2019), following the approach described by van de Plassche (1986) and Shennan (2015). To be considered as valid SLIP, any geological, sedimentary, or biological facies must have four main attributes:

1. An accurate geographic location.
2. An accurate elevation benchmarked to a tidal datum.
3. A well-constrained relationship between the sea-level indicator and paleo sea level.
4. The age of formation, traditionally obtained with radiometric dating techniques.

The database also includes limiting data points, which provide an upper (terrestrial limiting) or lower (marine limiting) bound against the past RSL position (Shennan, 2015; Khan et al., 2019).

For each SLIP and limiting data point, we refer to “Unique sample ID” of the record to collate the text to the database included in the Supplementary Information.

SLIPs and limiting data points were rejected when there was insufficient information. For example, when the depth of a sample within the core was reported but not the core top elevation, the data point was rejected. Marine samples with 14C age adjusted for Delta $R < 603$ were rejected because they were not valid for the calibration curve (Stuiver and Polach, 1977). Another reason for rejection was if a SLIP was at odds regarding the RSL estimate with coeval data points in the same region.

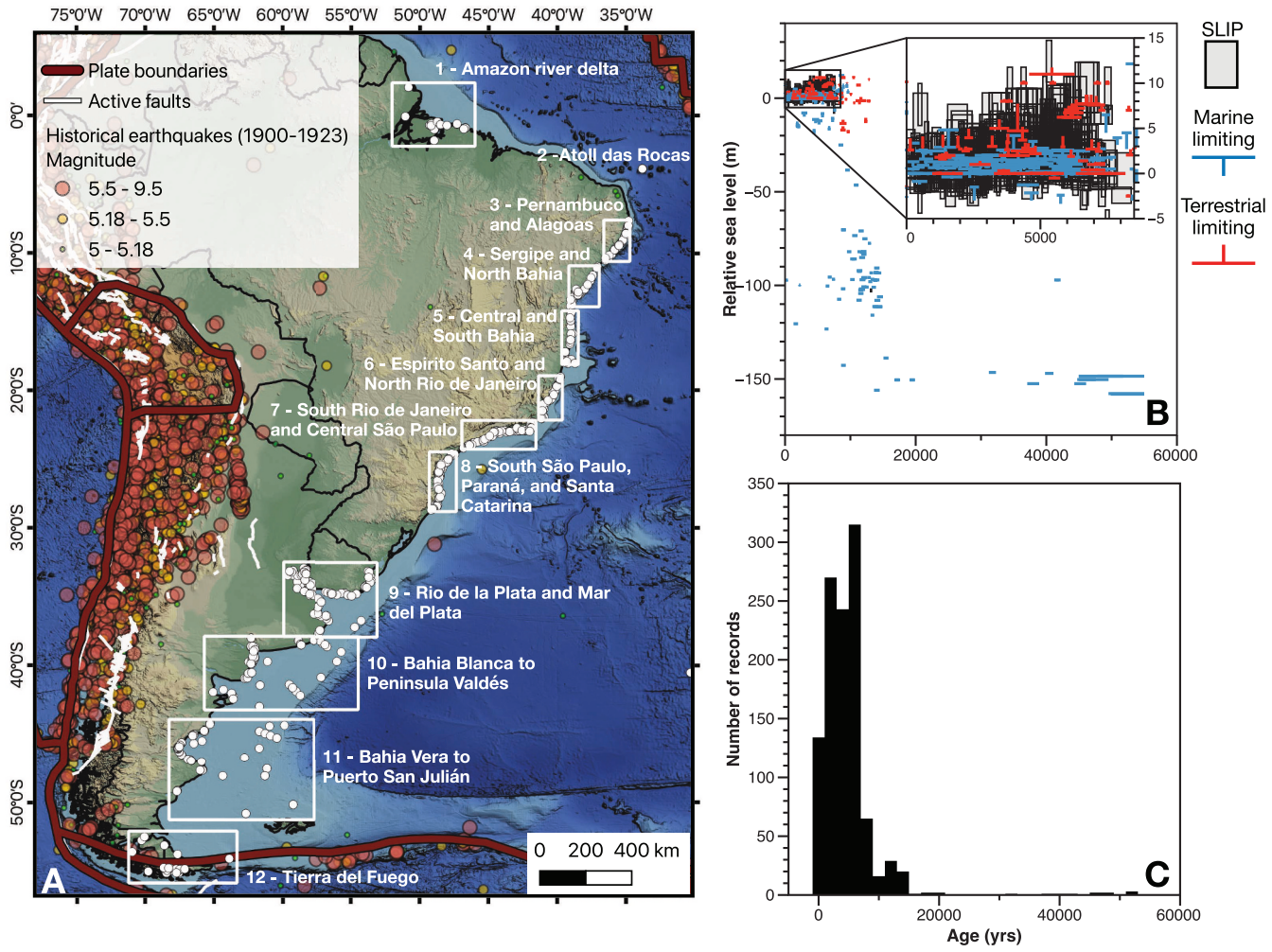

Fig. 1. Spatiotemporal extent of the sea-level database. A) Regional subdivisions described in the text. B) Age vs. RSL elevation plot for all the data points. C) Ages of the SLIPs included in the database. Credits: Base map from Ryan et al. (2009). Active faults from Styron (2019) and plate boundaries derived from Bird (2003), as modified by Hugo Ahlenius and Nordpil on GitHub (https://github.com/fraxen/tectonicplates). Historical earthquakes from US Geological Survey (2017).

Rejected data were not eliminated from the database and are available for future reassessment in case further information arises. The rejection of a SLIP does not reflect the quality of the published papers but rather the suitability of each record to be used to reconstruct RSL.

3.1. Location of sea-level index points

The locatons covered by the database spans between 0° and 60° latitude South and between 40° and 70° longitude West (Fig. 1A). We divided our database into 12 regions based on data availability, geographic distribution and the increasing distance from the Antarctic ice sheet. The location of individual SLIPs was determined via coordinates published in the original papers and, in case no coordinates were available, derived from maps in the original papers.

3.2. Elevation of sea-level index points

In the Holocene sea-level database for the Atlantic coasts of South America, we included the elevation of each SLIP and the defined vertical datum from the original works, wherever available (Table 1). We account for potential sources of error in the measurement of a sample elevation following the criteria described in the database protocol by Hijma et al. (2015) (Table 2). If either the measurement method or vertical datum was not reported, we set the elevation error to 20% of the measured elevation, with a lower error limit of 0.2 m (for elevations between −1 m and + 1 m) and an upper error limit of 2 m (for elevations higher than 10 m or deeper than −10 m). If neither the elevation measurement method nor the vertical datum was reported by the original publication, we set the elevation error to 40% of the measured elevation, with a lower error limit of 0.2 m (for elevations between −0.5 m and + 0.5 m) and an upper error limit of 2 m (for elevations higher than 5 m or deeper than −5 m).

Some studies, particularly those along the coasts of Patagonia, report elevations relative to the high tide level or “high tide mark”. In these instances, the reported elevation was corrected to mean sea level by subtracting the difference between the local Mean Higher High Water (MHHW) and Mean Lower Low Water (MLLW) calculated using the IMCalc software (Lorscheid and Rovere, 2019).

Several studies along the Brazilian coasts report paleo sea level as the vertical distance between the modern and the fossil populations, bypassing the need to report sample elevation (e.g., Angulo et al., 2006; Toniolo et al., 2020). As elevation of a sample is a required field in the HOLSEA standardized format, we considered these reported values as sample elevations and assigned a 40% uncertainty, as no other information was available on either the originally adopted indicative range or the originally measured elevation. A note was inserted in the record for each of these SLIPs indicating the use of vertical distance in the original publication. A 40% uncertainty was also assigned for the Argentinian data reported by Codignotto et al. (1992), as little information on the elevation measurement is provided in the paper and the

Table 1
Combinations of elevation measurement methods and vertical datums reported in the database.

Elevation measurement method	Vertical datum	Number of occurrences
Not reported	Not reported	360
	Mean Sea Level / General definition	222
	Mean sea level from tidal data	51
	Nazaré Pier	4
	Vermetid biological datum	153
Total station or Auto/hand level	High Tide Level	82
	Mean Sea Level / General definition	6
Differential GPS	Local geoid	24
	Mean sea level from tidal data	17
	EGM 2008	7
	SAD-69	6
Handheld GPS	Mean Sea Level / General definition	8
Topographic map and digital elevation models	Mean Sea Level / General definition	7
Barometric altimeter	Local geoid	12
	Mean sea level from tidal data	8
	High Tide Level	3
	Not reported	3
	Mean Sea Level / General definition	2
Multibeam bathymetry data + core depth	Mean Sea Level / General definition	103
	Not reported	23
Dumpy level	Vermetid biological datum	7

previous studies cited therein.

3.3. Indicative meaning of sea-level indicators

The indicative meaning of a sea-level indicator is the relationship of the local environment in which it accumulated to a contemporaneous reference tide level (Horton et al., 2000). Since sea-level trends are seldom inferred from a single type of dated material, and to allow for comparisons between different areas, each sample is related to its own Reference Water Level (RWL). The Indicative Range (IR) represents the vertical elevation range occupied by a sea-level indicator relative to contemporary tidal levels. The RWL is the midpoint of the IR.

We have reviewed all published evidence to allocate each SLIP with an indicative meaning (Figs. 2, 3, and Table 3). If the information provided in the original literature was insufficient to quantify the indicative meaning through direct comparison with a modern analog, we calculated it using the IMCalc software (Lorscheid and Rovere, 2019).

For beach ridges in Argentina and Uruguay, that are created by wave runup processes (Rovere et al., 2025), we calculated the indicative meaning using modern wave data and wave runup models to estimate their lower (ordinary berm) and upper limits (higher storm berm). Through this process, we calculated the 2% exceedance wave runup level using the different models implemented into the py-wave-runup tool coded by Leaman et al. (2020) following the methodology employed in Rubio-Sandoval et al. (2024).

The models used to calculate the indicative meaning of beach ridges require as input the beach slope, significant wave height, and period. As beach slope (tanβ), we used the values reported obtained by Rubio-Sandoval et al. (2024) for the beach of Camarones ($\tan\beta = 0.18 \pm 0.02$), which are representative of a reflective beach. These were obtained using the CoastSat.Slope toolbox (Vos et al., 2019, 2020), that analyzed Landsat and Sentinel satellite data between 2000 and 2023, alongside tides extracted from the FES2014 global tidal model (Lyard et al., 2021; Carrere et al., 2016). To calculate wave height and period we used the RADWave tool (Smith et al., 2020), which allows querying satellite altimetry data. We extracted a time series of wave data between 66°W to 70°W and 38°S to 52°S, in a period included between Jan 1st, 2000, and Jan 1st, 2023. For the same time frame, we queried the FES2014 model and extracted water levels at a 15-min interval. By coupling tidal and wave data via their UTC timestamps, we gathered a database with 231,462 wave conditions. For each of this condition, we selected a random beach slope sampled from a normal distribution created with the mean and standard deviation of the beach slope for each condition. We used the "ensemble" function of py-wave-runup to run for each wave height and period eight different runup models (Supplementary Fig. 1). We added (or subtracted) the corresponding water level to each calculated runup value.

Table 2
Sources of vertical uncertainties included in the database. Each vertical uncertainty was applied as appropriate to different samples. SLIP: Sea-Level Index Point; RTK GPS: Real-Time Kinematic Global Positioning System; DEM: Digital Elevation Models.

Core samples or sections	
Source of uncertainty	Description
Sample thickness uncertainty	Half of the sample thickness
Sampling uncertainty	Depth range of the dated sample
Core shortening/ stretching uncertainty	± 0.01 m if not specified ± 0.15 m for rotatory/vibracoring ± 0.05 m for hand coring ± 0.05 m for hand coring ± 0.01 m for Russian sampler Assigned largest uncertainty (± 0.15 m) if type of corer was unclear
Non-vertical drilling uncertainty	2% (e.g., 0.02 m/m depth)
Outcrops or other type of paleo-sea level indicators	
Tidal uncertainty (Applies only to samples collected offshore with reference to the water's surface)	Half of the tidal range
Water depth uncertainty	Uncertainty associated with the measurements of water depth, as reported ± 0.05 m if not specified
Levelling uncertainty	± 0.01 m for high-precision levelling equipment (e.g., total station, dumpy level) ± 0.03 m if levelling method is unknown, but the authors mentioned elevations measured/surveyed ± 20% or 40% of reported elevations if further uncertainties regarding the SLIP levelling
GPS or RTK uncertainty	Uncertainty associated with RTK GPS measurements, as reported ± 0.1 m if not specified
Benchmark uncertainty (Does not apply to samples that were not levelled to a benchmark)	± 0.1 m for reliable and stable benchmarks ± Precision of benchmarks if further uncertainties
Vegetation zone uncertainty (Applies only to samples whose elevations were estimated from vegetation zones)	± 20% of the reported elevation range of vegetation
Map uncertainty	± 0,50 m for high-precision levelling (additional elevation methods are included) ± 1 m if only a topographic map were used to determine sample elevation
DEM uncertainty	± 0,50 m (as recommended by Hijma et al., 2015 for areas with significant relief)

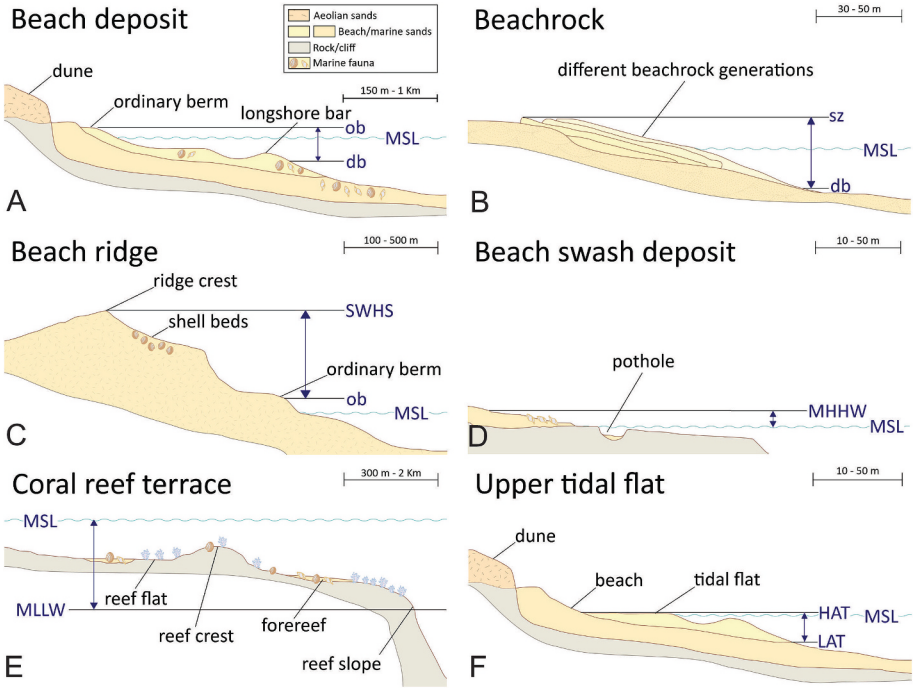

Fig. 2. Schematic illustration of the paleo-sea level indicators with their upper and lower limits of the Indicative Range shown by the black lines and blue arrows (see Table 1 for more details and definitions). A) to F) schemes of paleo-sea level indicators. db: breaking depth; ob: ordinary berm; sz surf zone; MSL: mean sea level; SWHS: storm wave swash height; MHHW: mean higher high water; MLLW: mean lower low water; HAT: highest astronomical tide; LAT: lowest astronomical tide. (For interpretation of the references to colour in this figure legend, the reader is referred to the web version of this article.)

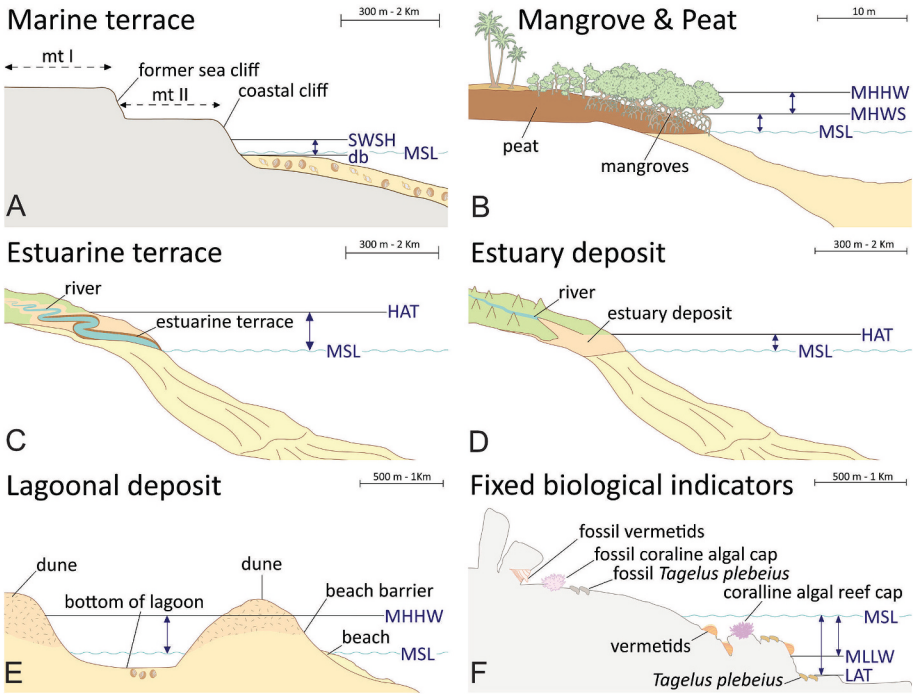

Fig. 3. Schematic illustration of the paleo-sea level indicators with their upper and lower limits of the Indicative Range shown by the black lines and blue arrows (see Table 1 for more details and definitions). A) to F) schemes of paleo-sea level indicators. mtI: marine terrace I; mtII: marne terrace II; db: breaking depth; ob: ordinary berm; sz: surf zone; MSL: mean sea level; SWHS: storm wave swash height; MHHW: mean higher high water; MHWS: mean high water springs; MLLW: mean lower low water; HAT: highest astronomical tide; LAT: lowest astronomical tide. (For interpretation of the references to colour in this figure legend, the reader is referred to the web version of this article.)

3.4. Radiometric ages

In the Holocene sea-level database for the Atlantic coasts of South America, the age of the samples was determined using radiocarbon dating (^{14}C). As the production of atmospheric radiocarbon has varied through geological time, we recalibrated all radiocarbon ages reported in the literature into sidereal years with a 2σ range. Age calibrations were done using CALIB software (version 8.2; Stuiver et al., 2021). We

Table 3
Types of paleo-sea level indicators in the database, including their indicative range and number of occurrences. MLLW = Mean Lower Low Water; MHHW = Mean Higher High Water; MSL = Mean Sea Level; LAT = Lowest Astronomical Tide; HAT = highest astronomical tide; MHWS = Mean High Water Springs; GWL = Groundwater Level. * Denotes indicative ranges provided by the revised publications.

Primary indicator type	Secondary indicator type	Indicative range	Number of occurrences
Beach deposit	Beach deposit or beachrock	Breaking depth to ordinary berm	68
		MLLW to MHHW*	1
	Beach ridge	Back calculated from values reported by the original authors*	51
		Ordinary berm to storm wave swash height	287
	Beach swash deposit	MHHW to MSL	1
Fixed biological indicators	Coral reef terrace or Coralline algal reef cap	MSL to MLLW	17
	Tagelus plebeius	LAT to MSL	2
	Vermetids	MLLW to MSL	177
Marine terrace	Marine Terrace	Breaking depth to storm wave swash height	33
Sedimentary	Basal Peat (non-mangrove)	MHHW to MSL	2
	Estuarine terrace (preserved tidal flat surface)	MSL to HAT	28
	Estuary deposit	HAT to MSL	2
	Lagoonal deposit	MHHW to MSL	2
	Mangrove	Measured on modern analog*	5
		MSL to MHWS	19
	Upper Tidal Flat	LAT to HAT	4
The data point is a marine or terrestrial limiting indicator		N/A	409

use the Marine20 curve to calibrate marine and estuarine samples (Heaton et al., 2020; Reimer et al., 2020), and the SHcal20 curve for terrestrial samples (Hogg et al., 2020). Marine reservoir corrections have been applied according to the closest available data for each study area (Macario et al., 2023). When a study site was in an area with unknown Delta-R values, we used the Marine Reservoir Correction Database (Reimer and Reimer, 2001). Following the analysis by Hu (2010) of 14C ages from bulk peat samples, a ± 100 14C yr error was applied to account for sample contamination (Törnqvist et al., 2015). Codignotto et al. (1992), Björck et al. (2021), and Fasano et al. (1983) reported calibrated ages. Therefore, we did not re-calibrate them. While their reported uncertainties are included and these data are kept in our database, caution should be exercised in their use as these ages are not directly comparable with the recalibrated data.

All SLIPs in our database are presented as calibrated years before present (years cal BP), where present refers to 1950 CE (Stuiver and Polach, 1977). A concern with old radiocarbon ages (i.e., dates determined before 1980) is the correction for isotopic fractionation (Törnqvist et al., 2015). This correction became a standard procedure at most laboratories by the late 1970s (Stuiver and Polach, 1977), but some laboratories have only applied this correction since the mid-1980s (Hijma et al., 2015). When needed, we applied the isotopic fractionation correction as reported by the authors. If the correction was not reported, we used the marine carbonate standard ±3 ‰ (Törnqvist et al., 2015). Further details and choices made while compiling the radiocarbon ages are available in the supplementary file.

3.5. Models of Holocene relative sea level change and glacial isostatic adjustment

To draw a continuous RSL curve for each region identified within the database (see sections 4.1 and 4.2 for details), we applied the Spatio-Temporal Empirical Hierarchical Model (STEHM) by Ashe et al. (2019) to the SLIPs.

We use GIA model RSL predictions forced by different ice models. We use the SELEN code to calculate RSL (Spada and Stocchi, 2007; de Boer et al., 2014, 2017). SELEN assumes the Earth's rheology is spherically symmetric with an elastic lithosphere and a Maxwell viscoelastic mantle and calculates sea level using a constant time step. This version of SELEN also considers migrating shorelines and Earth's rotational effects. In this study, we compute the sea level at 500-year time steps.

The first ice model we employ in our comparison is ICE-6G_C (VM5a) (hereafter referred to as ICE6G) (Argus et al., 2014; Peltier et al., 2015). The version of the model we use includes a global ice sheet history spanning the past 122,000 years. The time step for this model is not constant and is larger than 500 years prior to 21,000 years cal BP, so we linearly interpolate the ice sheet thickness between the time steps. The ice volume of the ICE6G model was tuned to a RSL record from Barbados (Fairbanks, 1989) and refined to fit present-day vertical land motion in areas covered by Late Pleistocene ice sheets. The VM5a Earth model that was used in conjunction with ICE6G has a 60 km thick lithosphere, a 40 km thick layer below the lithosphere with a viscosity of 1 × 1022 Pa s, a 5 × 1020 Pa s upper mantle, a 1.6 × 1021 Pa s lower mantle between 660 and 1160 km depth, and the rest of the lower mantle with a viscosity of 3.2 × 1021 Pa s. Peltier et al. (2015) used the Holocene sea-level indicators from southeastern South America, as compiled in Rostami et al. (2000), to evaluate the ICE6G model. They attributed the Holocene highstand position to rotational effects. By including rotational effects, the calculated sea level from ICE6G was better able to match the high-stand in many locations along the eastern South American coast. The Patagonian Ice Sheet in ICE6G has a sea level equivalent ice volume of 0.9 m at the LGM, which decreases to its present-day value at 15,500 years cal BP.

The second ice model we employ is the PaleoMIST 1.0 reconstruction (Gowan et al., 2021b). This model was designed as a preliminary ice sheet and topography reconstruction for the past 80,000 years, at 2500-year time steps. The Earth model used with PaleoMIST has a 120 km thick lithosphere, 4 × 1020 Pa s upper mantle, and 4 × 1022 Pa s lower mantle. The ice thickness has been linearly interpolated to 500-year time steps for the calculations in this study. The model was tuned with RSL observations from the Laurentide and Eurasian ice sheets, but it has not been extensively tested against far-field sea level records, such as those in eastern South America. Some initial calculations for southeastern South America reported by Gowan et al. (2021a) demonstrated that the sea level highstand may not have happened simultaneously along the coast. PaleoMIST 1.0 results show that the ice volume during the Mid to Late Holocene is too great to account for far-field sea level observations (Gowan, 2023b). Almost all this excess ice volume is in Antarctica. Therefore, in this paper, we have modified PaleoMIST 1.0 to use the present-day Antarctica ice sheet configuration from 5000 years cal BP to mitigate this issue. The Patagonian Ice Sheet in PaleoMIST has a sea level equivalent ice volume of 0.8 m at the LGM, which decreases to present-day values at 12,500 years cal BP.

4. Results

The Holocene sea-level database for the Atlantic coasts of South America consists of 1108 valid data points (701 SLIPs, 100 terrestrial and 307 marine limiting points) each associated with a temporal and vertical uncertainty. We rejected 291 data points because the necessary information required by the standard sea-level database protocols was not achieved.

The database spans the last 12,000 years cal BP, with nearly 80% of

the data younger than 10,000 years cal BP (Fig. 1C). Most radiocarbon age errors are lower than 500 years, and RSL elevation uncertainties (including elevation error and indicative meaning uncertainty) are between 0.5 m and 2 m.

4.1. Brazil

4.1.1. Region 1: Amazon river delta

The region encompassing the Amazon river delta area is located in northern Brazil, between Amapá and Pará states (Fig. 4A). Within this region, we gathered 27 SLIPs and 15 limiting data. The main SLIPs are derived from mangroves (Cohen et al., 2005; Behling et al., 2001),

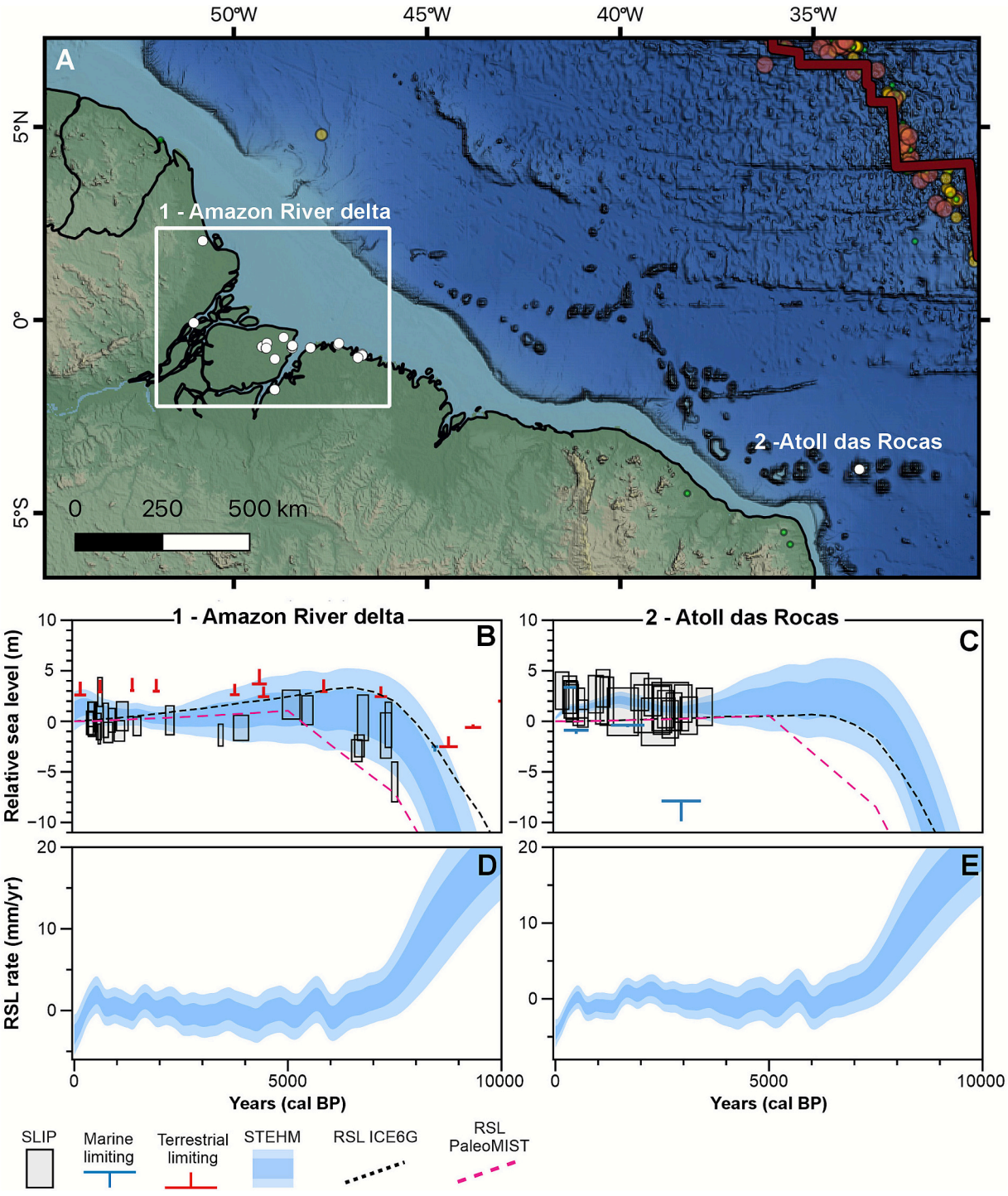

Fig. 4. Map (A) and RSL reconstructions (B-E) and rates from regions 1 and 2 using the spatio-temporal model. For all plots, the model mean and 2σ uncertainty are represented by a solid line and shaded envelopes, respectively. SLIPs (grey boxes) are plotted as calibrated age against RSL to the present. Limiting points are plotted as an "inverted-T" red symbol for terrestrial or an "T" blue symbol for marine. The dimensions of boxes and symbols for each point are based on elevation and age (2σ) errors. SLIP: sea-level index point; STEHM: spatio-temporal empirical hierarchical model; ICE6G (short, dashed line) and PaleoMIST (large, dashed line) represent the GIA models. Legend and credits for the base map in A) are the same as Fig. 1A. (For interpretation of the references to colour in this figure legend, the reader is referred to the web version of this article.)

estuarine deposits (Behling et al., 2004; Cohen et al., 2012), upper tidal flats (Cohen et al., 2012; Guimarães et al., 2012), and basal peat (non-mangrove) (Ribeiro et al., 2023).

The record in the Amazon River delta dates back to the Early Holocene (Fig. 4B). The oldest SLIP in this region places RSL at −6 ± 1.9 m at 7508 ± 76 years cal BP (Unique sample ID: 748). SLIPs indicate RSL rose to a peak at 1.6 ± 1.4 m at 5000 years cal BP (Fig. 4B). One SLIP (Unique sample ID: 734) documents a high RSL value of 2.9 ± 1.4 m at 614 ± 55 years cal BP.

The STEHM shows an increase in the RSL during the Mid-Holocene (from 8000 to 5000 years BP) at an average rate of 1.6 mm/yr. After 5000 years cal BP, the rate of RSL change slowly fell through the Late Holocene at a mean rate of 0.5 mm/yr (Fig. 4B, D). The GIA prediction from the ICE6G model fits the data, while PaleoMIST model seems to underestimate RSL at the beginning of the Mid-Holocene (Fig. 4B).

4.1.2. Region 2: Atol das Rocas

The Atol das Rocas is an atoll island located 250 km offshore the northeastern Brazilian coast. In this region we reviewed 25 SLIPs and 6 limiting data (Fig. 4C). The predominant paleo sea level indicators are coral reef terraces (Gherardi and Bosence, 2005) and beach deposits ((Angulo et al., 2022a). In addition, a single lagoonal deposit has been reported (Kikuchi and Leao, 1997).

In Atol das Rocas there is an absence of Early Holocene data. From 3000 years cal BP to the present, SLIPs are scattered both spatially and temporally, but indicate that the local sea level in this region was above present-day sea level, on average, +1.6 m (Fig. 4C).

The STEHM model shows a gradual decrease in relative sea level over the last 3000 years, with an average rate of about 0.5 mm/yr (Fig. 4C, E). GIA model predictions show that the sea level in this region was already close to its modern position around 5000 years cal BP, and GIA predictions are significantly lower than the observed RSL in the region, however remaining within the error bars of the SLIPs and the STEHM (Fig. 4C).

4.1.3. Region 3: Pernambuco and Alagoas

In this region, we reviewed 31 SLIPs, and 33 limiting data (Fig. 5B). Vermetid rims are the dominant paleo-sea level indicators (Martin et al., 1996; Dominguez et al., 1990; Angulo et al., 2006). Other indicators include beach deposits (Dominguez et al., 1990), mangroves (Barbosa et al., 1986), and a coralline algal reef cap (Delibrias and Laborel, 1971; Laborel, 1969).

The records in Pernambuco and Alagoas date back to the Mid-Holocene. The oldest SLIP (Unique sample ID: 143) places RSL at 0.3 ± 1.9 m at 7896 ± 619 years cal BP. Younger SLIPs indicate RSL rose to ca. 5 m ± 1.8 m at 3800 years cal BP (Fig. 5B).

According to the STEHM, after the Mid-Holocene RSL highstand (around 6000 years cal BP), RSL falls to its present-day position at a mean rate of 0.5 mm/yr (Fig. 5B, E). The GIA prediction from the model ICE6G fits the data, while PaleoMIST seems to underestimate the RSL at the beginning of the Mid-Holocene (Fig. 5B).

4.1.4. Region 4: Sergipe and North Bahia

In the Sergipe and North Bahia region, we reviewed 35 SLIPs, and 16 limiting data (Fig. 5C). In this region, there are three types of paleo-sea level indicators: vermetid rims (Bittencourt et al., 1978; Martin et al., 1979; Delibrias and Laborel, 1971; Angulo et al., 2006), beach deposits (Bittencourt et al., 1978; Martin et al., 1979), and mangroves (Martin et al., 1979; Martin et al., 1982).

The records in Sergipe and North Bahia date back to the Early Holocene. The oldest SLIP (Unique sample ID: 152) places the RSL at −2.4 ± 0.8 m at 8028 ± 362 years cal BP (Fig. 5C). From there, the RSL increases to ~1.7 ± 1.9 m ca. 5700 years cal BP. One data point (Unique sample ID: 211) stands out, recording the highest RSL value of 5 ± 1.9 m at 5462 ± 357 years cal BP. However, this unusually high value appears inconsistent with the general trend and should be carefully re-evaluated to confirm its reliability. Younger SLIPs in this region plot RSL between ~3 to ~2 m between 4000 and 2000 years BP, after which it falls close to its modern position (Fig. 5C).

According to the STEHM RSL rose between 6000 and 4300 years BP, with rates of change gradually decreasing. During the Late Holocene, RSL showed a general trend toward stabilization with minor fluctuations and lower rates of change (Fig. 5C, F). The GIA prediction from the model ICE6G fits the data, while PaleoMIST seems to underestimate the RSL at the beginning of the Mid-Holocene (Fig. 5C).

4.1.5. Region 5: Central and South Bahia

In the region encompassing Bahia state's central and southern sectors, we reviewed 37 SLIPs and 20 limiting data (Fig. 5D). The sea-level indicators identified in this region consist of beach deposits (Angulo et al., 2022b), vermetid rims (Bittencourt et al., 1978; Martin et al., 1979; Martin et al., 1996; Angulo et al., 2006, 2022b), and mangroves (Fontes et al., 2017; Cohen et al., 2020).

The record of this region dates to the Mid-Holocene. RSL changes in this region show slight oscillations over time, with values ranging from 4 m to −0.9 m. Two data points (Unique sample IDs: 249; 1214) show the highest RSL values (4.3 ± 1.6 m and 4.5 ± 1. 7 m, respectively) at around 5000 years cal BP (Fig. 5D).

The STEHM shows a rising sea level between 8000 and 4000 years BP with a mean rate of change of 1.8 mm/yr. From the Late Holocene onward, sea level gradually fell, marking a slow regression (Fig. 5D, G). The GIA model predictions of ICE6G show a good agreement with the RSL history reconstructed by the STEHM, while PaleoMIST underestimates the trend at the beginning of the Mid-Holocene (Fig. 5D).

4.1.6. Region 6: Espírito Santo and North Rio de Janeiro

Twelve SLIPs and 48 limiting data were reviewed in this region (Fig. 6B). Therefore, RSL history of this region is based primarily on limiting data (Delibrias and Laborel, 1971; Martin and Suguio, 1989; Martin et al., 1996; Martin et al., 1997). The few SLIPs identified include vermetid rims (Martin and Suguio, 1989; Martin et al., 1996; Angulo et al., 2006, 2016), and one associated with a beach deposit (Martin et al., 1996; Martin et al., 1997).

The record of this region dates back to the Mid-Holocene. The marine limiting data suggests that RSL was already above present-day sea level at 7000 years cal BP. The oldest SLIP (Unique sample ID: 347) places the sea level at 1.7 ± 0.6 m at 6019 ± 781 years cal BP. Sea level reached a peak of 3.6 ± 1.3 m around 5000 years cal BP. RSL oscillated around an average level of 3 m until 3000 years cal BP after which it began a falling trend to the present (Fig. 6B).

The STEHM shows a rising sea level between 8000 and 5000 years BP. During this period, the rate of RSL change reaches a maximum, with an average value of approximately 1.7 mm/yr. After this rise, the RSL falls into the Late Holocene (Fig. 6B, E). ICE6G GIA predictions fit the data, while PaleoMIST predictions are lower until ca. 5000 years cal BP (Fig. 6E).

4.1.7. Region 7: South Rio de Janeiro and Central São Paulo

In this region, we reviewed 62 SLIPs and 47 limiting data (Fig. 6C). Despite the large number of SLIPs, only two types of indicators were described in this region: vermetid rims (Delibrias and Laborel, 1971; Martin and Suguio, 1978; Suguio and Martin, 1978; Flexor and Martin, 1979; Martin et al., 1979;; Suguio et al., 1980; Martin et al., 1996; Angulo et al., 2006; Castro et al., 2014; Angulo et al., 2016; Babtista de Jesus et al., 2017; Castro et al., 2021), and beach deposits (Martin et al., 1979; Martin and Suguio, 1989; Angulo et al., 2006; Castro et al., 2014; Angulo et al., 2016; Castro et al., 2021).

The record in this region mainly corresponds to the Mid-Holocene. There are only two marine limiting data from the Early Holocene, which indicate a sea level of ca. -15 m (Fig. 6C). The Mid-Holocene data suggest that from 7000 to 5000 years BP, sea level was close to the present-day mean sea level, averaging ~1.1 m. Just one SLIP (Unique

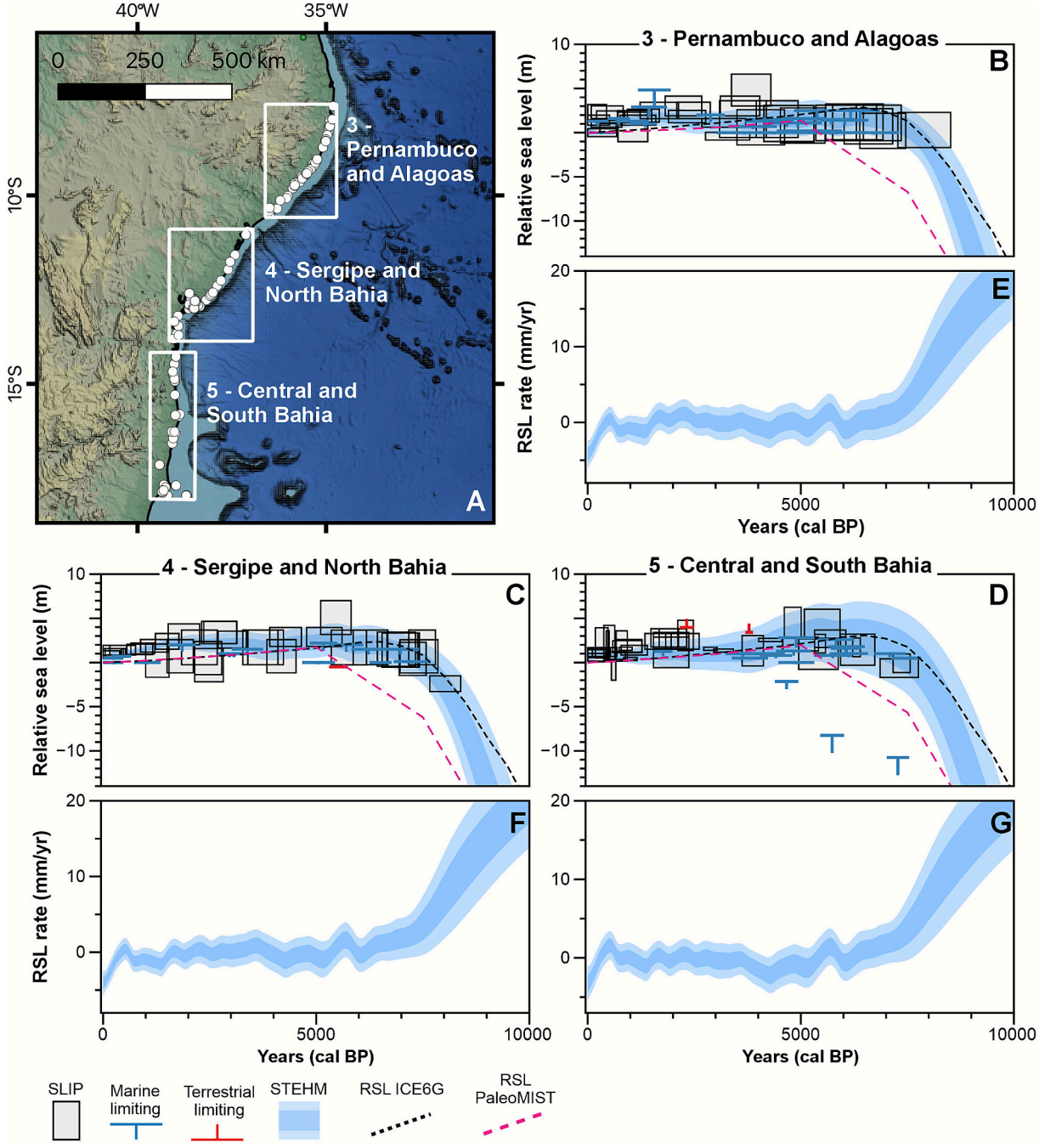

Fig. 5. Map (A) and RSL reconstructions (B-G) and rates from regions 3, 4, and 5 using the spatio-temporal model. For all plots, the model mean and 2σ uncertainty are represented by a solid line and shaded envelopes, respectively. Index points (grey boxes) are plotted as calibrated age against changes in sea level relative to the present. Limiting points are plotted as an "inverted-T" red symbol for terrestrial or an "T" blue symbol for marine. The dimensions of boxes and symbols for each point are based on elevation and age (2σ) errors. SLIP: sea-level index point; STEHM: spatio-temporal empirical hierarchical model; ICE6G (short, dashed line) and PaleoMIST (large, dashed line) represent the GIA models. Legend and credits for the base map in A) are the same as Fig. 1A. (For interpretation of the references to colour in this figure legend, the reader is referred to the web version of this article.)

sample ID: 464) shows a higher RSL value (2.3 ± 1.5 m) at 5834 ± 276 years cal BP. This regional record shows Mid-Holocene sea level peaked at4900 years cal BP at 3.8 ± 1.4 m. Still, one SLIP (Unique sample ID: 463) indicates a higher RSL (4.7 ± 2.2 m) at 3370 ± 243 years cal BP. After this time, RSL falls gradually toward its modern position (Fig. 6C).

The STEHM shows a rapid sea level rise between 8000 and 6000 years BP, with rates peaking around 7.2 mm/yr, followed by a gradual deceleration in sea level rise from 6000 to 4000 years BP. During the Late Holocene, RSL stabilizes near present-day levels, with rates fluctuating around zero (Fig. 6C, F). ICE6G GIA predictions fit the data, while PaleoMIST predictions are lower than the observed RSL values at the beginning of the Mid-Holocene (Fig. 6C).

4.1.8. Region 8: South São Paulo, Paraná, and Santa Catarina

In South Sao Paulo, Parana, and Santa Catarina states, we reviewed 61 SLIPs and 32 limiting points (Fig. 6D). All the reported paleo-sea level indicators in this region are vermetid rims (Angulo, 1989, 1992; Angulo et al., 1999; Souza et al., 2001; Angulo et al., 2002; Toniolo et al., 2020; Angulo et al., 2022c).

The record in South Sao Paulo, Parana, and Santa Catarina date back

to the Mid-Holocene. The oldest SLIP (Unique sample ID: 544) places the sea level at 2.3 ± 0.8 m at 5685 ± 228 years cal BP. The highest sea level value is observed around 5000 years cal BP at ca. 3.8 ± 1. 4 m. Since then, the RSL gradually falls toward the present-day sea level, ranging from ~3.3 ± 1.0 m to ~0.4 ± 0.3 m (Fig. 6D).

The STEHM shows a rapid RSL rise culminating in a highstand around 6000 years cal BP, with rates reaching up to ~5 mm/yr. Following this highstand, the RSL progressively falls during the Late Holocene, with rates gradually decreasing from ~1 mm/yr to near 0 by 2000 years cal BP (Fig. 6D, G). The ICE6G GIA model predictions fit the data, whereas PaleoMIST predictions are lower than the RSL trend described by the STEHM during the beginning of the Mid-Holocene (Fig. 6D).

4.2. *Uruguay – Argentina*

4.2.1. *Region 9: Río de la Plata delta*

In this region, we reviewed 169 SLIPs and 28 limiting data (Fig. 7B).

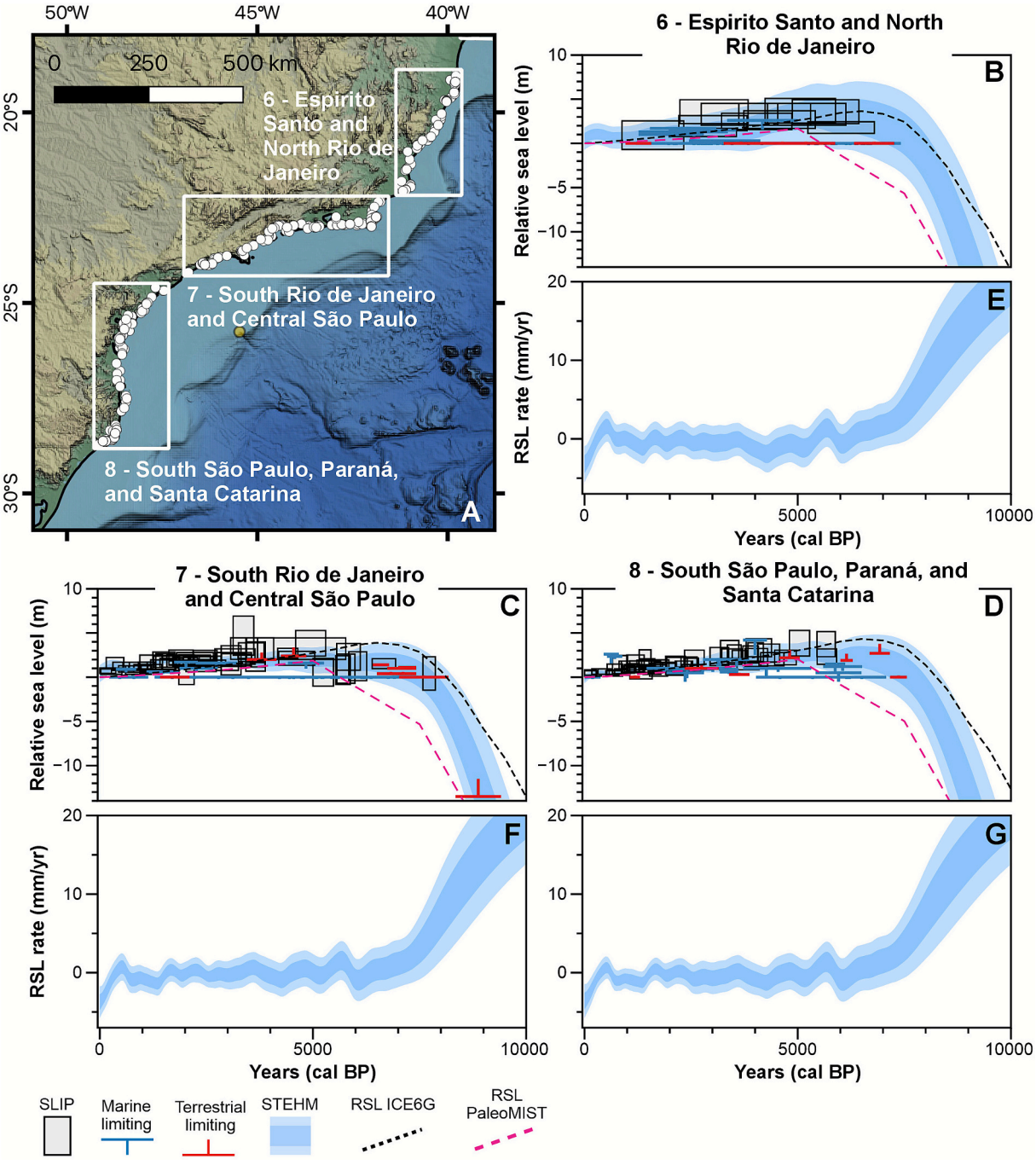

Fig. 6. Map (A) and RSL reconstructions (B-G) and rates from regions 6, 7, and 8 using the spatio-temporal model. For all plots, the model mean and 2σ uncertainty are represented by a solid line and shaded envelopes, respectively. Index points (grey boxes) are plotted as calibrated age against changes in sea level relative to the present. Limiting points are plotted as an "inverted-T" red symbol for terrestrial or an "T" blue symbol for marine. The dimensions of boxes and symbols for each point are based on elevation and age (2σ) errors. SLIP: sea-level index point; STEHM: spatio-temporal empirical hierarchical model; ICE6G (short, dashed line) and PaleoMIST (large, dashed line) represent the GIA models. Legend and credits for the base map in A) are the same as Fig. 1A. (For interpretation of the references to colour in this figure legend, the reader is referred to the web version of this article.)

The main paleo-sea level indicators described in the region were beach ridges (Cortelezzi, 1977; Albero and Angiolini, 1983; Guida and González, 1984; Codignotto et al., 1992; Cortelezzi et al., 1992; Aguirre, 1993; Colado et al., 1995; Cavallotto, 1995; Cavallotto, 2002; Bracco and Ures, 1998; Bracco, 2000; Bracco et al., 2011; Martínez and Rojas, 2013; Prieto et al., 2017; Cavallotto et al., 2004; Cavallotto et al., 2005; Martínez et al., 2006) and estuary deposits (Albero and Angiolini, 1983; Fasano et al., 1983; González and Ravizza, 1987; Figini, 1992; Martínez et al., 2006; Amato and Busso, 2009; Prieto et al., 2017; Fucks and De Francesco, 2003). One upper tidal flat deposit, one beach swash deposit (Bracco and Ures, 1998; Prieto et al., 2017), and two biological indicators (deposits containing remnants of the mollusk *Tagelus plebeius*) were also described (Bracco et al., 2011).

The record in Rio de la Plata delta mainly corresponds to the Mid-Holocene, only one terrestrial limiting data suggests that RSL was −18 m during the Early Holocene (Supplementary Fig. 2). The oldest SLIP (Unique sample ID: 296) places the sea level around 3.1 ± 0.6 m at 6800 ± 480 years cal BP. Two SLIPs (Unique sample IDs: 47; 269) show the highest RSL value ~4.7 m at 5398 ± 187 years cal BP and 4991 ± 476 years cal BP, respectively. Since then, the data shows an almost

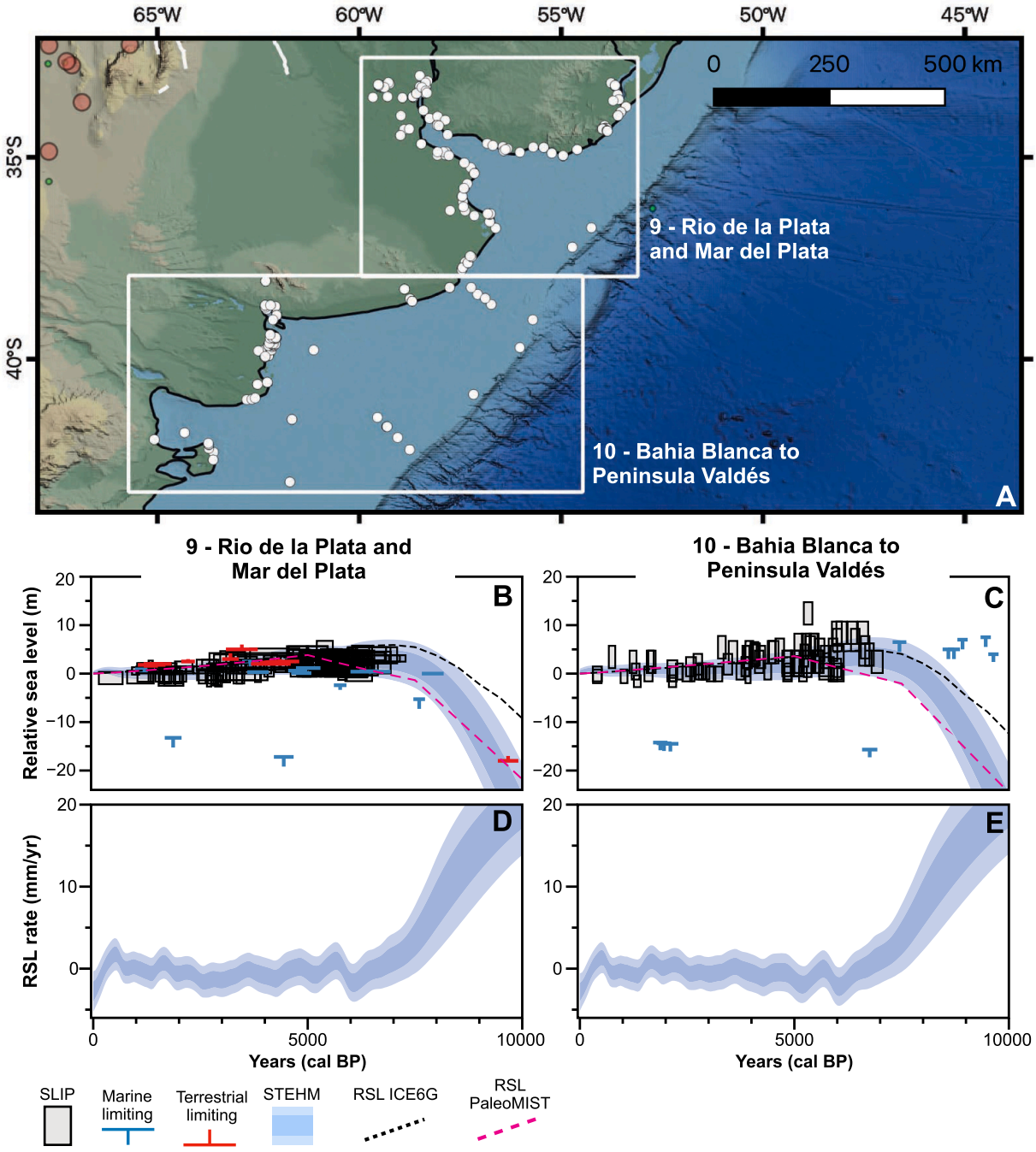

Fig. 7. Map (A) and RSL reconstructions (B-E) and rates from regions 9 and 10 using the spatio-temporal model. For all plots, the model mean and 2σ uncertainty are represented by a solid line and shaded envelopes, respectively. Index points (grey boxes) are plotted as calibrated age against changes in sea level relative to the present. Limiting points are plotted as an "inverted-T" red symbol for terrestrial or an "T" blue symbol for marine. The dimensions of boxes and symbols for each point are based on elevation and age (2σ) errors. SLIP: sea-level index point; STEHM: spatio-temporal empirical hierarchical model; ICE6G (short, dashed line) and PaleoMIST (large, dashed line) represent the GIA models. Legend and credits for the base map in A) are the same as Fig. 1A. (For interpretation of the references to colour in this figure legend, the reader is referred to the web version of this article.)

continuous RSL fall (Fig. 7B).

According to the STEHM, RSL reached its highstand around 7000 years cal BP, followed by a progressive fall with rates decreasing from about 3.7 mm/yr to near 0. During the Late Holocene, the RSL continued to decline, but at much slower and more variable rates (Fig. 7B, D). Both GIA models fit the data from 8000 years cal BP to the present day (Fig. 7B).

4.2.2. Region 10: Bahia Blanca to Peninsula Valdés

In the region from Bahia Blanca to Peninsula Valdes, we reviewed 85 SLIPs and 31 limiting data points (Fig. 7C). Only two types of paleo-sea level indicators are reported along these coasts: beach ridges (Codignotto et al., 1992) and marine terraces (Rostami et al., 2000). Most marine data points derive from sediment cores collected on the Argentine shelf (Guilderson et al., 2000).

In this region, as in Region 9, data from the Early Holocene is represented by limiting points (Supplementary Fig. 2). The oldest SLIP (Unique sample ID: 1147) places the sea level at 2.4 ± 2.3 m at 6930 ± 130 years cal BP. Since then, RSL values oscillate, ranging from 8.4 ± 2.3 m to −1.57 ± 1.2 m. However, a general trend of RSL fall after a Mid-Holocene highstand is observed. One SLIP (Unique sample ID: 1164) shows the highest RSL value (12.4 ± 2.3 m) around 5320 ± 100 years cal BP (Fig. 7C). However, this value seems at odds with the sea level trend during that time and this SLIP needs further examination.

According to the STEHM, the RSL record shows rising sea level, with rates up to 17.7 mm/yr, from 9500 to 7000 years BP, followed by a gradual fall toward the present-day sea level (Fig. 7C, E). Comparing GIA models' predictions with the data, both models fit the data from 8000 years cal BP to the present day (Fig. 7C).

4.2.3. Region 11: Bahia Vera to Puerto San Julián

The region from Bahia Vera to Puerto San Julián includes an extensive coastline from the center of Chubut Province to the south of Santa Cruz Province in Argentina. Here, we reviewed 132 SLIPs and 69 limiting data (Fig. 8B). The most common indicators in the region are beach ridges (Codignotto et al., 1992; Schellmann, 2007; Schellmann and Radtke, 2010; Ribolini et al., 2011; Zanchetta et al., 2012; Zanchetta et al., 2014); although marine terraces (Rostami et al., 2000; Schellmann and Radtke, 2000, 2003, 2010; Schellmann, 2007), estuarine deposits (Bini et al., 2018), and one upper tidal flat (Desiage et al., 2023) are also described.

The records in Bahia Vera and Puerto San Julián date back to the Early Holocene (Supplementary Fig. 2). The oldest SLIP (Unique sample ID: 1444) places the RSL at −102 ± 0.7 m at 13165 ± 78 years cal BP. Since then, the dataset shows scattered SLIPs with values ranging from 9 m to −1.0 m. However, an RSL falling trend is observed (Fig. 8B).

The STEHM, the RSL record shows a rising RSL from around 9000 to approximately 7000 years BP, reaching a Mid-Holocene highstand at a mean rate of about 11.2 mm/yr. Following the highstand, the RSL gradually declined toward the present-day sea level (Fig. 8B, D). As in the previous region, both GIA models fit the data from 8000 years cal BP onward (Fig. 8B).

4.2.4. Region 12: Tierra del Fuego

In the southernmost region, we reviewed 37 SLIPs and 62 limiting data (Fig. 8C). The indicators described are beach ridges (Rabassa et al., 2000; Codignotto et al., 1992; Gordillo et al., 1993; Bujalesky, 2007; Isla and Bujalesky, 2008), marine terraces (Gordillo et al., 1993; Bujalesky, 2007; Isla and Bujalesky, 2008), beach deposits (Porter et al., 1984), basal peat (non-mangrove) (Porter et al., 1984; Gordillo et al., 1993; Bujalesky, 2007; Isla and Bujalesky, 2008), and lagoon deposits (Björck et al., 2021).

The SLIPs data mainly corresponds to the Mid-Holocene. However, some limiting data shows an Early Holocene age (Supplementary Fig. 2). The oldest SLIP (Unique sample ID:983) places the RSL at 1.9 ± 2.1 m ca. 6259 ± 333 years cal BP. SLIPs between 5700 and 4400 years BP show variability in sea level between ~1.6 and ~ 4.6 m with peaks at 5700 (6.0 m) and 4400 (4.6 m). Overall, the data shows a general trend of sea level fall from the peak at about 5700 years cal BP toward the present, with a slight rise observed in the last ~50 years (Fig. 8C).

The STEHM shows a Mid-Holocene highstand occurring roughly between 9000 and 7000 years BP, with relative sea level rates peaking around 17.7 mm/yr. Following this highstand, the rates gradually decline, transitioning through near zero values around 3000 years cal BP reaching a long-term relative sea-level fall with rates up to 3.3 mm/yr (Fig. 8C, E). In this region, both GIA models fit the data since the Mid-Holocene (Fig. 8C).

5. Discussion

5.1. Methods to build a Holocene relative sea-level database

Holocene RSL data were compiled from a diverse range of indicators, including beach deposits, sedimentary sequences, and fixed biological indicators. Our results show generally good agreement with RSL reconstructions derived from different indicators across most regions. However, in regions 1 and 3, we observed that RSL estimates based on sedimentary sequences are up to ~1 m lower than those derived from other indicators. This discrepancy may be due to post-depositional lowering from compaction processes (Khan et al., 2022). Compaction distorts stratigraphy and lowers RSL reconstruction relative to their depositional altitudes. This compaction-driven post-depositional lowering can lead to misinterpretation of the magnitude and rate of reconstructed RSL change, potentially resulting in misattribution of RSL drivers (Törnqvist et al., 2004; Horton and Shennan, 2009). Despite this, our reconstructed RSL histories align well with previous compilations (e.g., Angulo et al., 2006; Milne et al., 2005; Fig. 9A, B), further confirming that standardizing sea-level data can yield coherent results, even when different methods are used to quantify the indicative meaning of SLIPs.

In the Holocene sea-level database for the Atlantic coasts of South America, vermetid rims from Brazil constitute the majority of data points (e.g., Codignotto et al., 1992; Martin et al., 1996; Cavallotto, 2002; Angulo et al., 2006, 2022b; Bracco et al., 2011; Martínez and Rojas, 2013). We note that some sources of vertical error and uncertainty associated with these indicators could affect the reported RSL interpretations. For example, Laborel (1986) notes that wave energy can shift the vertical distribution of vermetids by approximately 1 m. Angulo et al. (1999) identify three additional sources of uncertainty when using vermetid fossils to infer paleo-sea level: (i) the remains may not correspond to the upper limit of formation, (ii) the coastal hydrodynamic regime may have changed over time, and (iii) the vertical reference used to assess the displacement of vermetid reefs may be uncertain. Rovere et al. (2015) emphasize that most vermetid species have a broad living range, which can be narrowed when specific biological associations are considered, as illustrated by Angulo et al. (2022c). To standardize the vertical distribution and uncertainty of these indicators in our database, we adopted a general indicative range (MSL to MLLW) and defined an *ad hoc* datum (vermetid biological datum).

Paleo tidal range changes may also influence the indicative meaning of SLIPs whose vertical bounds are tied to tidal levels (e.g., Hill et al., 2011; Hall et al., 2013; Horton et al., 2013; Khan et al., 2017; Sulzbach et al., 2023). For beach ridges, in this work, we follow the interpretation of Lorscheid and Rovere (2019) and Rovere et al. (2016), who suggest that they form above sea level, between the ordinary berm and the storm wave swash height, consistent with Tamura's (2012) definition of gravel beach ridges. According to this definition, MHHW is used to estimate both the ordinary berm and storm wave swash heights (Lorscheid and Rovere, 2019). Paleo tidal range changes may therefore be particularly relevant in areas with wide continental shelves, such as the Amazon River and Rio de la Plata deltas, and Bahia Blanca. In this study, we used satellite-derived wave measurements and wave runup models to calculate the indicative meaning of beach ridges, following the methodology

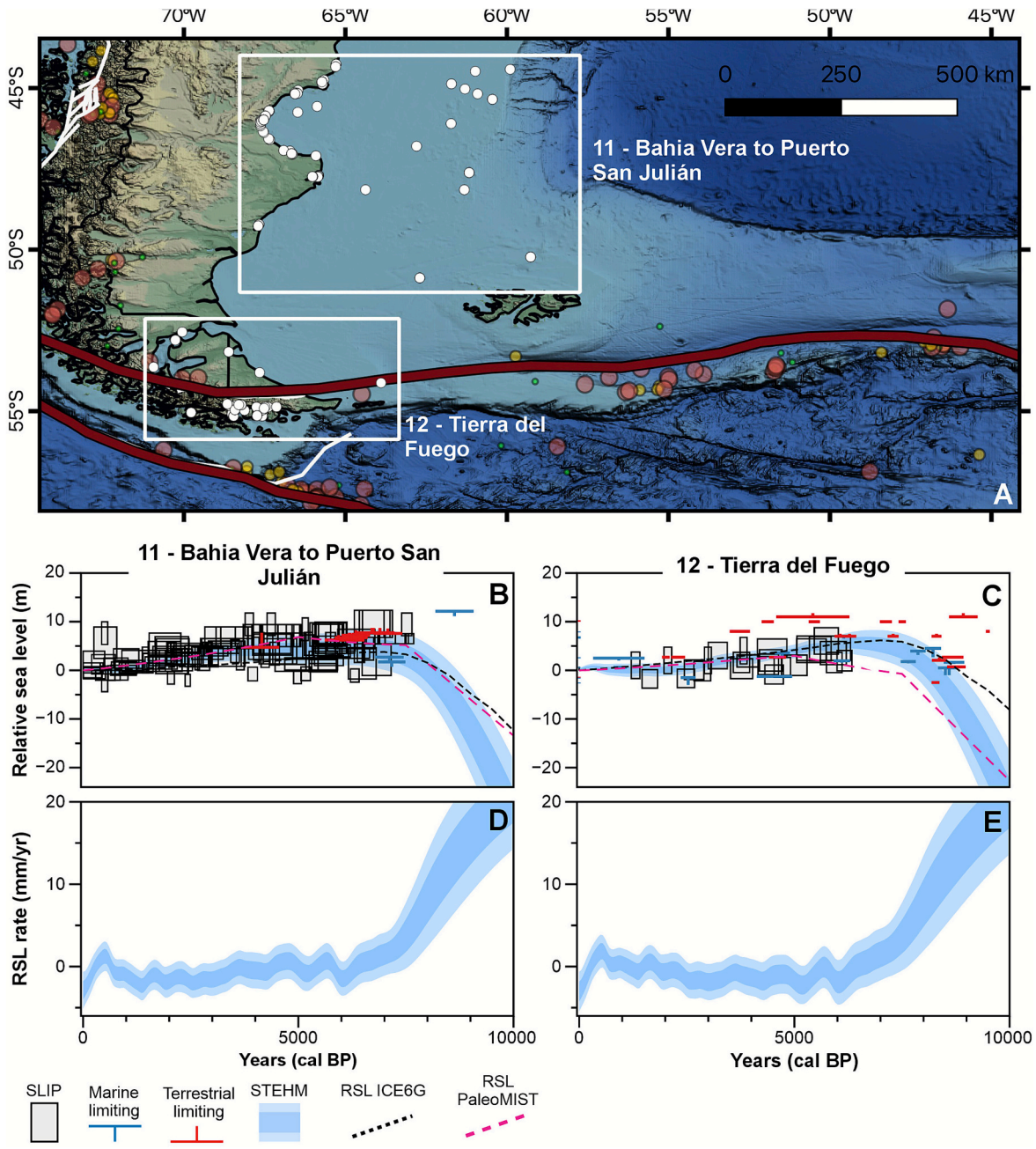

Fig. 8. Map (A) and RSL reconstructions (B-E) and rates from regions 11, and 12 using the spatio-temporal model. For all plots, the model mean and 2σ uncertainty are represented by a solid line and shaded envelopes, respectively. Index points (grey boxes) are plotted as calibrated age against changes in sea level relative to the present. Limiting points are plotted as an "inverted-T" red symbol for terrestrial or an "T" blue symbol for marine. The dimensions of boxes and symbols for each point are based on elevation and age (2σ) errors. SLIP: sea-level index point; STEHM: spatio-temporal empirical hierarchical model; ICE6G (short, dashed line) and PaleoMIST (large, dashed line) represent the GIA models. Legend and credits for the base map in A) are the same as Fig. 1A. (For interpretation of the references to colour in this figure legend, the reader is referred to the web version of this article.)

of Rubio-Sandoval et al. (2024). While this approach does not resolve uncertainties related to paleo tidal ranges (as it does not take into account changes in shelf bathymetry), it incorporates local wave and beach topography data and appears more reliable than the IMCalc software (Lorscheid and Rovere, 2019), which relies on global wave atlases and generalized beach slope values (Rovere et al., 2025).

5.2. Holocene RSL variability along the Atlantic coasts of South America

We reconstructed Holocene RSL histories to capture regional RSL variations along the Atlantic coastlines of Brazil, Uruguay, and Argentina (Figs. 4, 5, 6, 7, and 8). In general, observed and predicted RSL changes show a rising trend between 8000 and 5000 years BP, with a mean rate of 1.7 mm/yr (Angulo and Camargo Lessa, 1997; Angulo et al., 2006; Schellmann and Radtke, 2010). This culminated in a highstand of ~2 to ~4 m above present-day sea-level, followed by a gradual fall to modern levels. Given the broad spatial extent of the study area, this Mid- to Late Holocene trend is variably influenced by ice and ocean mass redistribution, and in some cases, by local crustal tectonics (Rostami et al., 2000; Milne et al., 2005).

In northern Brazil, estuarine deposits and mangroves from the Amazon River delta record a Mid-Holocene highstand of ~2 m above sea level. After this highstand, RSL declined during the Late Holocene at a mean rate of −1.3 mm/yr (Fig. 4D). This trend, excluding Atol das

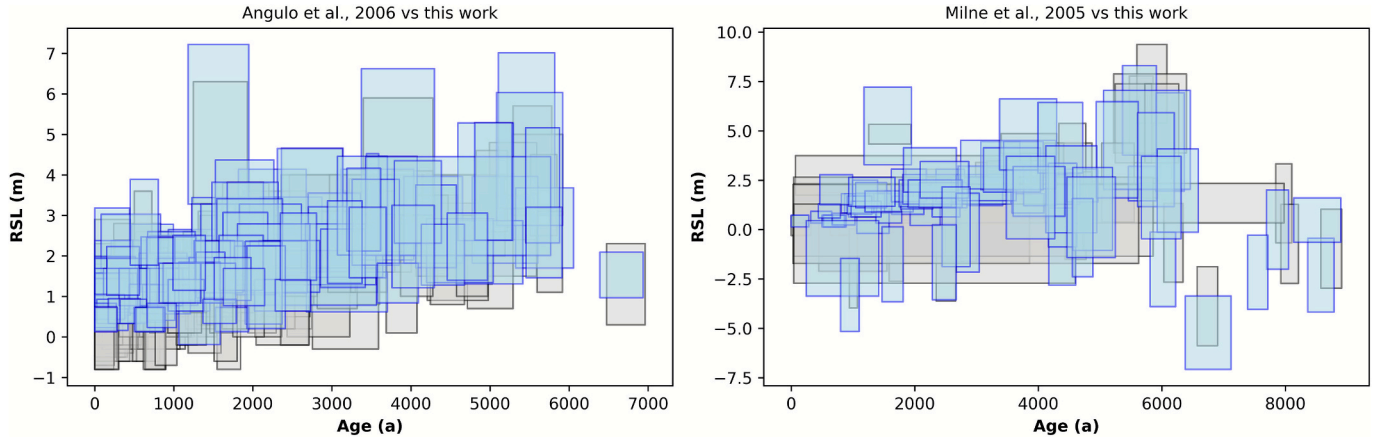

Fig. 9. Comparison between our data (blue) and the standardized data of A) Angulo et al. (2006) and B) Milne et al. (2005) (grey). (For interpretation of the references to colour in this figure legend, the reader is referred to the web version of this article.)

Rocas, differs from the rest of the northeastern sector. Regions from Pernambuco to northern Bahia show a highstand of ~5 m between 6000 and 4000 years BP, followed by a fall in RSL toward present-day levels at a mean rate of 0.5 mm/yr. As noted by Angulo et al. (2006), SLIPs from mangrove swamp deposits in northern Brazil suggest a lower RSL than expected, indicating that neotectonics and wind-wave dynamics may influence the RSL trend in this area. Additionally, the effects of sedimentary compaction may alter the elevation of RSL (Törnqvist et al., 2004; Horton and Shennan, 2009). Therefore, interpretations of RSL in the Amazon delta estuarine region should be approached with caution, and further work is needed to quantify the role of compaction.

The scattered data in Atol das Rocas (Fig. 6E) may reflect palaeoceanographic changes, which introduce vertical uncertainties in coral reef SLIPs (Shennan et al., 2018; Khan et al., 2019). As hydrodynamic conditions such as waves, weather, and tides, affect the growth patterns of coralline-algal reefs, which may interfere with RSL reconstructions (Angulo et al., 2022a), leading to histories that deviate from regional expectations.

In the region covering the Brazilian states from Sergipe to Bahia, a second RSL highstand is observed between 4000 and 2000 years BP (Fig. 5). The presence of Late Holocene RSL oscillations in Brazil has long been debated (Angulo and Camargo Lessa, 1997; Martin et al., 1998, 2003; Angulo et al., 2006). However, more precise indicators are required to test the hypothesis of a second Holocene highstand and also of Holocene sea-level oscillations.

The southeastern coastal region of Brazil, from Espirito Santo to Santa Catarina, shows a coherent Holocene RSL trend (Fig. 6). RSL rose rapidly from 8000 years cal BP, with maximum rates of up to 7 mm/yr but averaging ~3 mm/yr overall. This sea-level rise culminated in a Mid-Holocene highstand of ~3 to 4.7 m above present-day levels between 6000 and 5000 years BP. Following this highstand, RSL gradually declined at average rates up to ~ − 0.3 mm/yr, reaching near-modern levels in the Late Holocene. These trends align with the global ice-equivalent (eustatic) sea-level pattern described by Milne et al. (2005), who reported a rapid Early Holocene RSL rise (~7–8 mm/yr) followed by deceleration. Leading to the Mid-Holocene highstand and subsequent gradual Late Holocene RSL fall. Moreover, the observed regional trends are consistent with GIA model predictions, particularly the ICE6G model, highlighting the importance of isostatic processes in shaping Holocene RSL history in southeastern coastal region of Brazil.

Between the Rio de la Plata delta and Tierra del Fuego, the Mid-Holocene highstand occurred slightly earlier (from 7000 to 6000 years BP) than in northern regions and was similarly followed by a Late Holocene sea-level fall. However, highstand elevations vary across this extensive coastal stretch between 35°S and 55°S (Figs. 7 and 8). Milne et al. (2005) proposed that the observed differences in highstand elevations reflect a temporal offset, resulting from the combined effect of West Antarctic ice sheet meltwater redistributing the geoid during the Early Holocene and from crustal subsidence in some parts of the region. They also note that various processes can cause vertical movement of both land and ocean surfaces, leading to a significant component of RSL change and, consequently, to variability in observed RSL values.

In addition to these differences in highstand elevation, the SLIP data between Rio de la Plata and Tierra del Fuego are notably scattered both spatially and temporally (Figs. 7 and 8). This may reflect differences in geomorphological settings and dating uncertainties. Schellmann and Radtke (2010) suggest that discrepancies in RSL change along the Patagonian Atlantic coast may stem from gaps in geomorphological and chronostratigraphic records, compounded by variable ^{14}C reservoir effects that produce unquantifiable age uncertainties. We applied local Delta-R corrections where possible to reduce these errors. However, the lack of such correction data for Argentinean Patagonia limits interpretability, and these data should be treated cautiously.

In Tierra del Fuego, RSL reconstructions are likely shaped by GIA (Björck et al., 2021, and localized tectonic activity (Isla and Angulo, 2016; Rostami et al., 2000). Björck et al. (2021) argue that GIA, driven by the Patagonian Ice Sheet, is the dominant factor behind the elevated shorelines and the spatial–temporal variability of RSL in this area. In contrast, Rostami et al. (2000) contend that the Patagonian Ice Sheet (estimated to have a maximum thickness of ~400 m; Hulton et al., 1994) would not have produced a significant RSL response along the Argentinean coast. Rostami et al. (2000) show that, contrary to expectations of forebulge collapse and sea-level rise, Holocene terraces in the region are uplifted rather than submerged, implying that localized tectonic uplift may have played a more important role then GIA. They estimate a consistent uplift rate of 0.09 m/1000 yr in Patagonia since the Mid-Pleistocene. Before a unique RSL history for this region can be established, limitations in both spatial and temporal data coverage, and an improved understanding of glacial history must be addressed.

The influence of GIA across the broad latitudinal range covered by our database is evident in both the data and the STHEM model (Figs. 4, 5, 6, 7, and 8). Generally, the Holocene highstand occurs later and with lower magnitude toward the north, following patterns predicted by GIA models. As shown by Peltier et al. (2015), highstand elevations in many locations can be reproduced by the ICE6G model, which incorporates rotational effects into RSL calculations. The modified PaleoMIST model used in this study does not match data older than 5000 years cal BP, suggesting that global ice volume at 7500 years cal BP may be overestimated by 4–5 m sea-level equivalent. The model's good performance after 5000 years cal BP supports the interpretation that Antarctic ice volume had reached near-present-day levels by that time.

Although this study does not aim to extrapolate the revised Holocene

RSL curves to a broader regional scale, some comparisons are warranted. Despite uncertainties, the RSL reconstructions presented here align with expected trends for both near-field and far-field settings, with a few exceptions already discussed. The data from Tierra del Fuego, a near-field location due to its proximity to Antarctica, show a complex RSL fall following a highstand, shaped by the combined effects of global mean sea-level rise and glacio-isostatic uplift (Milne and Mitrovica, 2008). In contrast, regions from the Rio de la Plata delta (Uruguay) to the Amazon delta (Brazil) exhibit far-field RSL behavior. These large-scale patterns are broadly consistent with the classical GIA zones of Clark and Lingle (1979), which predict lower-amplitude, subsidence-tending Holocene responses along far-field continental margins and more complex signals toward southern near-field areas affected by Antarctic loading. Our latitudinal database refines these first-order predictions by revealing marked along-shore variability, (particularly in northeastern Brazil) where local processes modulate the GIA signal.

Enhancing the quality of RSL data in this region and integrating it with standardized datasets from intermediate-field areas (e.g., the Caribbean, Khan et al., 2017) and northern near-field sites (e.g., Atlantic USA, Engelhart and Horton, 2012; Southern Maine, Khan et al., 2015; Gulf of Maine, Baril et al., 2023; Canada, Vacchi et al., 2018; Greenland, Gowan, 2023a, 2023b), would support the development of a comprehensive pole-to-pole sea-level dataset. Such a dataset would improve GIA model calibration and yield more robust estimates of global mean sea-level change since the LGM.

6. Conclusions

We present the first standardized database of Holocene RSL for the southwestern Atlantic. The database includes over 1108 data points from Brazil, Uruguay, and Argentina, with 701 SLIPs, 100 terrestrial limiting points, and 307 marine limiting points. An additional 291 data points were excluded due to missing information required by standard protocols. This work also underscores the importance of methodologically consistent approaches (especially in the treatment of complex indicators like vermetids and beach ridges) for generating reliable RSL reconstructions.

Despite the regional variability and occasional data gaps, our compilation reveals coherent RSL histories that highlight the interplay between ice equivalent sea level glacio-isostatic adjustment, sediment compaction, and local tectonics across more than 50 degrees of latitude.

Our findings confirm a consistent Mid-Holocene highstand ranging from ~2 to ~4 m above present-day, followed by a gradual fall toward modern levels. There is a latitudinal gradient in highstand timing and magnitude (i.e., highstand occurs later and with lower magnitude toward the north), which is consistent with GIA model predictions. However, the poor PaleoMIST model–data agreement before 5000 years cal BP calls for revised estimates of global ice volume in Early Holocene scenarios in this model.

While challenges remain in underrepresented regions such as Patagonia and the Amazon River delta, our database provides a robust foundation for future improvements. This standardized RSL database bridges a critical gap in the global sea-level record. When combined with similar efforts in the Caribbean and higher-latitude regions, it will enable the development of integrated pole-to-pole sea-level reconstructions, an essential step toward enhancing GIA models and constraining global mean sea-level budgets since the LGM.

CRediT authorship contribution statement

K. Rubio-Sandoval: Writing – original draft, Data curation, Conceptualization. **T.A. Shaw:** Writing – review & editing, Methodology, Data curation. **M. Vacchi:** Writing – review & editing, Methodology, Data curation. **N. Khan:** Writing – review & editing, Methodology, Formal analysis, Data curation. **B.P. Horton:** Writing – review & editing, Methodology, Conceptualization. **J.R. Angulo:** Writing – review & editing, Methodology, Data curation. **M. Pappalardo:** Writing – review & editing, Methodology, Data curation. **A.L. Ferreira-Júnior:** Writing – review & editing, Methodology, Data curation. **S. Richiano:** Writing – review & editing, Methodology, Data curation. **M.C. de Souza:** Writing – review & editing, Methodology, Data curation. **P.C. Giannini:** Writing – review & editing, Methodology, Data curation. **D.D. Ryan:** Writing – review & editing, Data curation, Conceptualization. **E.J. Gowan:** Writing – review & editing, Formal analysis, Data curation. **A. Rovere:** Writing – original draft, Project administration, Methodology, Formal analysis, Conceptualization.

Declaration of competing interest

On behalf of the co-authors, I certify that we have NO affiliations with or involvement in any organization or entity with any financial interest (such as honoraria; educational grants; participation in speakers' bureaus; membership, employment, consultancies, stock ownership, or other equity interest; and expert testimony or patent-licensing arrangements), or non-financial interest (such as personal or professional relationships, affiliations, knowledge or beliefs) in the subject matter or materials discussed in this manuscript.

Data availability

The authors confirm that all data necessary for supporting the scientific findings of this paper have been provided.

Acknowledgments

This work is part of the PhD thesis of Karla Rubio-Sandoval, funded by the European Research Council (ERC) under the European Union's Horizon 2020 research and innovation program (grant agreement no. 802414). This paper reflects only the author's view and that the EU is not responsible for any use that may be made of the information it contains. Karla Rubio-Sandoval also acknowledges the Monika Segl program of MARUM, Bremen University, for additional support. She also thanks the Instituto de Geociencias and DGAPA (Dirección General de Asuntos del Personal Academico) for the postdoctoral fellowship that was essential to complete the publication of this work. Timothy Adam Shaw and Ben Horton were supported by the Singapore Ministry of Education Academic Research Fund MOE2019-T3-1 004. We would like to thank Abdulla S. Khan for technical support during the development of the database and Lic. Ricardo Briseño López for his guidance in the design of the illustrations. We thank the PALSEA working group for the useful discussions during the 2022 meeting in Singapore. PALSEA is a working group of the International Union for Quaternary Sciences (INQUA) and Past Global Changes (PAGES), which in turn received support from the Swiss Academy of Sciences and the Chinese Academy of Sciences. We sincerely thank the reviewers for their constructive comments and suggestions, which significantly helped to improve the quality and clarity of this manuscript. Fig. 1 was created using ArcGIS® software by Esri. ArcGIS® and ArcMap™ are the intellectual property of Esri and are used herein under license ©Esri. All rights reserved. For more information about Esri® software, please visit https: //www.esri.com (last access: 20.06.2023). The data used in this study were compiled in WALIS, a sea-level database interface developed by the ERC Starting Grant WARMCOASTS (ERC-StG-802414) in collaboration with the PALSEA working group. The database structure was designed by Alessio Rovere, Deirdre D. Ryan, Thomas Lorscheid, Andrea Dutton, Peter Chutcharavan, Dominik Brill, Nathan Jankowski, Daniela Mueller, Melanie Bartz, Evan Gowan, and Kim Cohen. The beta-version of the WALIS data insertion interface for Holocene sea-level data was coded thanks to partial support by a PAGES Data Stewardship Scholarship. The authors used ChatGPT (OpenAI) to improve the clarity and readability of some paragraphs in the Discussion section. The authors reviewed and verified all content to ensure accuracy and scientific integrity.

Appendix A. Supplementary data

Supplementary data to this article can be found online at https://doi.org/10.1016/j.gloplacha.2026.105315 and the complete database is available open-access via Zenodo (https://doi.org/10.5281/zenodo.10819555) (Version 2.0; Rubio-Sandoval et al., 2025). If you use the database, we ask to cite not only this compilation, but the original works referred in this manuscript and in the database.

References

Aguirre, M.L., 1993. Palaeobiogeography of the Holocene molluscan fauna from Northeastern Buenos Aires Province, Argentina: its relation to coastal evolution and sea level changes. Palaeogeogr. Palaeoclimatol. Palaeoecol. 102, 1–26.

Albero, M.C., Angiolini, F.E., 1983. Ingeis Radiocarbon Laboratory Dates. Radiocarbon 831–842.

Amato, S., Busso, A.S., 2009. Estratigrafía Cuaternaria del subsuelo de la cuenca inferior del Río Paraná. Rev. Asoc. Geol. 64 (4), 594–602.

Angulo, R.J., 1989. Fossil vermetidae between latitudes 25° 34′ S and 27° 09S state of Paraná and state of Santa Catarina- Brazil. In: International symposium on global changes in South America during the Quaternary: Past- Present- Future, pp. 263–268.

Angulo, R.J., 1992. Ambientes de sedimentação planície costeira com cordões litorâneos no estado do Paraná. Boletin Paranaense de Geociências 40, 69–114.

Angulo, R.J., Camargo Lessa, G., 1997. The Brazilian sea-level curves: a critical review with emphasis on the curves from the ParanaguA and Canan&a regions. Mar 140 (1–2), 141–166.

Angulo, R.J., Giannini, P.C., Suguio, K., Pessenda, L.C., 1999. Relative sea-level changes in the last 5500 years in southern Brazil (Laguna–Imbituba region, Santa Catarina State) based on vermetid 14C ages. Mar. Geol. 159 (1–4), 323–339.

Angulo, R.J., Pessenda, L., Souza, M.C., 2002. O significado das datações ao 14C na reconstrução de paleoníveismarinhos e na evolução das barreiras Quaternárias do litoral paranaense. Revista Brasileira de Geociências 32, 95–106.

Angulo, R.J., Lessa, G.C., de Souza, M., 2006. A critical review of mid-to late-Holocene Sea-level fluctuations on the eastern Brazilian coastline. Quat. Sci. Rev. 25, 486–506.

Angulo, R.J., Giannini, P.C.F., De Souza, M.C., Lessa, G.C., 2016. Holocene paleo-sea level changes along the coast of Rio de Janeiro, southern Brazil: comment on Castro et al. (2014). An. Acad. Bras. Cienc. 88, 2105–2111. https://doi.org/10.1590/0001-3765201620140641.

Angulo, R.J., de Souza, M.C., da Camara Rosa, M.L.C., Caron, F., Barboza, E.G., Costa, M. B.S.F., Macedo, E., Vital, H., Gomes, M.P., Garcia, K.B.L., 2022a. Paleo-sea levels, Late-Holocene evolution, and a new interpretation of the boulders at the Rocas Atoll, southwestern Equatorial Atlantic. Mar. Geol. 447. https://doi.org/10.1016/j.margeo.2022.106780.

Angulo, R.J., de Souza, M.C., da Camara Rosa, M.L.C., Barboza, E.G., Lessa, G.C., Pessenda, L.C.R., Ferreira Junior, A.L., 2022b. Mid- to late Holocene Sea level changes at Abrolhos Archipelago and Bank, southwestern Atlantic Brazil. Mar. Geol. 450. https://doi.org/10.1016/j.margeo.2022.106841.

Angulo, R.J., de Souza, M.C., Giannini, P.C.F., Dillenburg, S.R., Barboza, E.G., da Camara Rosa, M.L.C., Hesp, P.A., Pessenda, L.C.R., 2022c. Late-Holocene Sea levels from vermetids and barnacles at Ponta do Papagaio, 27° 50′ S latitude and a comparison with other sectors of southern Brazil. Quat. Sci. Rev. 286, 107536.

Argus, D.F., Peltier, W.R., Drummond, R., Moore, A.W., 2014. The Antarctica component of postglacial rebound model ICE-6G_C (VM5a) based upon GPS positioning, exposure age dating of ICE thicknesses, and relative sea level histories. Geophys. J. Int. 198 (1), 537–563.

Ashe, E.L., Cahill, N., Hay, C., Khan, N.S., Kemp, A., Engelhart, S.E., Horton, B.P., Parnell, A.C., Kopp, R.E., 2019. Statistical modeling of rates and trends in Holocene relative sea level. Quat. Sci. Rev. 204, 58–77.

Babtista de Jesus, P., Dias, F.F., Muniz, R.D.A., Macário, K.C.D., Seoane, C.S., Quattrociocchi, D.G.S., Tardin, R.C., Aguilera, O., Correa, R.C., Queiroz, E., Silva, I., Alves, C.R., Araujo, J.C., 2017. Holocene paleo-sea level in southeastern Brazil: an approach based on vermetids shells. J. Sedim. Environ. 2 (1), 35–48.

Backeuser, E., 1918. A Faixa litorânea Do Brasil Meridional. Ontem ehoje. Tyy, Besnard Frêres, Rio de Janeiro, 207p.

Barbosa, L.M., Bittencourt, A.C.D.A., Dominguez, J.M., Martin, L., 1986. The Quaternary coastal deposits of the State of Alagoas: influence of the relative sea-level changes. Quaternary of South America and Antarctic Peninsula. 269–290.

Baril, A., Garrett, E., Milne, G.A., Gehrels, W.R., Kelley, J.T., 2023. Postglacial relative sea-level changes in the Gulf of Maine, USA: Database compilation, assessment and modelling. Quat. Sci. Rev. 306, 108027.

Barreto, A.M.F., Bezerra, F.H.R., Suguio, K., Tatumi, S.H., Yee, M., Paiva, R.P., Munita, C. S., 2002. Late Pleistocene marine terrace deposits in northeastern Brazil: sea-level change and tectonic implications. Paleogeography, Paleoclimatology, Paleoecology 179, 57–69.

Behling, H., Cohen, M.C.L., Lara, R.J., 2001. Studies on Holocene mangrove ecosystem dynamics of the Bragança Peninsula in North-Eastern Pará, Brazil. Palaeogeography, Palaeockimatology, Palaeoecology 167, 225–242.

Behling, H., Cohen, M.C.L., Lara, R.J., 2004. Late Holocene mangrove dynamics of Marajó Island in Amazonia, northern Brazil. Veg. Hist. Archaeobotany 13, 73–80. https://doi.org/10.1007/s00334-004-0031-1.

Bezerra, F.H.R., Vita-Finzi, C., 2000. How active is a passive margin? Paleoseismicity in northeastern Brazil. Geology 591–595.

Bini, M., Isola, I., Zanchetta, G., Pappalardo, M., Ribolini, A., Ragaini, L., Baroni, C., Boretto, G., Fuck, E., Morigi, C., Salvatore, M.C., Bassi, D., Marzaioli, F., Terrasi, F., 2018. Mid-Holocene relative sea-level changes along Atlantic Patagonia: New data from Camarones, Chubut, Argentina. Holocene 28, 56–64. https://doi.org/10.1177/0959683617714596.

Bird, P., 2003. An updated digital model of plate boundaries. Geochem. Geophys. Geosyst. 4 (3).

Bittencourt, A.D.S., Martin, L., Vilas Boas, G.D.S., Flexor, J.M., 1978. Quaternary marine formations of the coast of the state of Bahia (Brazil). In: Proceedings of 1978 International Symposium on Coastal Evolution in the Quaternary, pp. 232–253.

Björck, S., Lambeck, K., Möller, P., Waldmann, N., Bennike, O., Jiang, H., Li, D., Sandgren, P., Nielsen, A.B., Porter, C.T., 2021. Relative Sea level changes and glacio-isostatic modelling in the Beagle Channel, Tierra del Fuego, Chile: Glacial and tectonic implications. Quat. Sci. Rev. 251, 106–657.

Bracco, R., 1991. Dataciones 14C en Sitios con Elevación. Rev. Antropología, año 1, *I*, 11–17.

Bracco, R., 2000. Aproximación al registro arqueológico del sitio La Esmeralda ("conchero") desde su dimensión temporal. Anales de Arqueología y Etnología 54–55.

Bracco, R., Ures, M.C., 1998. Las variaciones del nivel del mar y el desarrollo de las culturas prehistóricas del Uruguay. Revista do Museu de Arqueologia e Etnologia 8, 109–115.

Bracco, R., García-Rodríguez, F., Inda, H., del Puerto, L., Castiñeira, C., Penario, D., 2011. Niveles relativos del mar durante el Pleistoceno final-Holoceno en la costa de Uruguay. In: El Holoceno En La Zona Costera de Uruguay, pp. 65–92.

Branner, J.C., 1889. The geology of Fernando de Noronha. Am. J. Sci. 37, 145–161.

Branner, J.C., 1890. The aeolian sandstones of Fernando de Noronha. Am. J. Sci. 39, 247–257.

Branner, J.C., 1902. Geology of northeast coast of Brazil. Bull. Geol. Soc. Am. 13, 41–98.

Branner, J.C., 1904. The stone reef of Brazil, their geological and geographical relations, with a chapter on the coral reefs. In: Bulletin of the Museum of Comparative Zoology at Harvard College v. 44, Geological Series v. 7. Cambridge, Massachuset, U.S.A, 285p. 99.

Bujalesky, 2007. Coastal Geomorphology and Evolution of Tierra del Fuego (Southern Argentina).

Carrere, L., Lyard, F., Cancet, M., Guillot, A., Picot, N., 2016. Fes2014, a new tidal model–validation results and perspectives for improvements, presentation to esa living planet conference.

Castro, J.W.A., Suguio, K., Seoane, J.C.S., Da Cunha, A.M., Dias, F.F., 2014. Sea-level fluctuations and coastal evolution in the state of Rio de Janeiro, southeastern Brazil. An. Acad. Bras. Cienc. 86, 671–683. https://doi.org/10.1590/0001-3765201420140007.

Castro, A., Wagner, J., Sicoli, S., Fernandes, D., Cabral, C., Meneguci da Cunha, A., Malta, J., Miguel, L., Areia de Oliveira, C., Spotorno de Oliveira, P., de Souza, Tapajós, Tamega, F., 2021. Relative Sea-level curve during the Holocene in Rio de Janeiro, Southeastern Brazil: a review of the indicators - RSL, altimetric and geochronological data. J. S. Am. Earth Sci. 112. https://doi.org/10.1016/j.jsames.2021.103619.

Cavallotto, J.L., 1995. Evolución geomorfológica de la Llanura Costera Ubicada en el Margen Sur del Río de la Plata. Universidad Nacional de La Plata.

Cavallotto, J.L., 2002. Evolución holocena de la llanura costera del margen sur del Río de la Plata. Rev. Asoc. Geol. Argent. 57, 376–388.

Cavallotto, J.L., Violante, R.A., Parker, G., 2004. Sea-level fluctuations during the last 8600 years in the de la Plata river (Argentina). Quat. Int. 114, 155–165. https://doi.org/10.1016/S1040-6182(03)00050-8.

Cavallotto, J.L., Violante, R.A., Colombo, F., 2005. Evolución Y Cambios Ambientales de la Llanura Costera de la Cabecera del río de la Plata.

Clark, J.A., Lingle, C.S., 1979. Predicted relative sea-level changes (18,000 years BP to present) caused by late-glacial retreat of the Antarctic ice sheet. Quat. Res. 11 (3), 279–298.

Codignotto, J.O., Kokot, R.R., Marcomini, S.C., 1992. Neotectonism and Sea-Level changes in the Coastal Zone of Argentina, Source. J. Coast. Res. 125–133.

Cohen, M.C.L., Behling, H., Lara, R.J., 2005. Amazonian mangrove dynamics during the last millennium: the relative sea-level and the Little Ice Age. Rev. Palaeobot. Palynol. 136, 93–108. https://doi.org/10.1016/j.revpalbo.2005.05.002.

Cohen, M.C.L., Pessenda, L.C.R., Behling, H., de Fátima Rossetti, D., França, M.C., Guimarães, J.T.F., Friaes, Y., Smith, C.B., 2012. Holocene palaeoenvironmental history of the Amazonian mangrove belt. Quat. Sci. Rev. 55, 50–58. https://doi.org/10.1016/j.quascirev.2012.08.019.

Cohen, M.C., Figueiredo, B.L., Oliveira, N.N., Fontes, N.A., França, M.C., Pessenda, L.C., de Souza, A.V., Macario, K., Guiannini, P.C.F., Bendassolli, J.A., Lima, P., 2020. Impacts of Holocene and modern sea-level changes on estuarine mangroves from northeastern Brazil. Earth Surf. Process. Landf. 45 (2), 375–392.

Colado, U., Figini, A., Fidalgo, F., Fucks, E., 1995. Los depósitos Marinos del Cenozoico Superior Aflorantes en la Zona Comprendida Entre Punta Indio Y el río Samborombón, Provincia de Buenos Aires.

Cortelezzi, C.R., 1977. Datacion de las formaciones marinas en el Cuaternario en las proximidades de la Plata-Magdalena, Providencia de Buenos Aires. Anales del Laboratorio de Ensayo de Materiales e Investigaciones Tecnológicas 75–93.

Cortelezzi, C.R., Pavlicelic, R.E., Pitori, C.A., Parodi, A.V., 1992. Variaciones del nivel del mar en el Holoceno en los alrededores de La Plata y Berisso. Actas IV Reunión Argentina de Sedimentología, La Plata 2, 131–138.

Darwin, C., 1851. Geological Observations on Coral Reefs, Volcanic Islands, and on South America: Being the Geology of the Voyage of the Beagle, under the Command of Captain Fitzroy, RN, during the Years 1832 to 1836. Smith, Elder.

Davies, B.J., Darvill, C.M., Lovell, H., Bendle, J.M., Dowdeswell, J.A., Fabel, D., García, J. L., Geiger, A., Glasser, D.M.G., Harrison, A.S.H., Kaplan, M.R., Martin, J.R.V., Mendelova, M., Palmer, A., Pelto, M., Rodés, E.A.S., Smedley, R.K., Thorndycraft, V. R., 2020. The evolution of the Patagonian Ice Sheet from 35 ka to the present day (PATICE). Earth-Sci. Rev. 204, 103152.

de Boer, B., Stocchi, P., Van De Wal, R., 2014. A fully coupled 3-D ice-sheet-sea-level model: algorithm and applications. Geosci. Model Dev. 7, 2141–2156.

de Boer, B., Stocchi, P., Whitehouse, P.L., van de Wal, R.S., 2017. Current state and future perspectives on coupled ice-sheet – sea-level modelling. Quat. Sci. Rev. 169, 13–28.

Delibrias, C., Laborel, J., 1971. Recent variations of the sea level along the Brazilian Coast. Quaternaria 45–49.

Desiage, P.A., St-Onge, G., Duchesne, M.J., Montero-Serrano, J.C., Haller, M.J., 2023. Late Pleistocene and Holocene transgression inferred from the sediments of the Gulf of San Jorge, Central Patagonia Argentina. J. Quat. Sci. 38 (5), 629–646.

Dominguez, J.M.L., Bittencourt, A.C.S.P., Leão, Z.M.A.N., Azevedo, A.E.G., 1990. Geologia do Quaternário costeiro do estado de Pernanbuco. Revista Brasileira de Geociências 20.

Düsterhus, A., Rovere, A., Carlson, A.E., Horton, B.P., Klemann, V., Tarasov, L., Barlow, N.L.M., Bradwell, T., Clark, J., Dutton, A., Roland Gehrels, W., Hibbert, F.D., Hijma, M.P., Khan, N., Kopp, R.E., Sivan, D., Törnqvist, T.E., 2016. Palaeo-sea-level and palaeo-ice-sheet databases: Problems, strategies, and perspectives. Clim. Past 12, 911–921. https://doi.org/10.5194/cp-12-911-2016.

Engelhart, S.E., Horton, B.P., 2012. Holocene Sea level database for the Atlantic coast of the United States. Quat. Sci. Rev. 54, 12e25. https://doi.org/10.1016/j.quascirev.2011.09.013.

Fairbanks, R.G., 1989. A 17,000-year glacio-eustatic sea level record: influence of glacial melting rates on the Younger Dryas event and deep-ocean circulation. Nature 342 (6250), 637–642.

Fasano, J., Ilsa, F., Schnack, E., 1983. Un análisis comparativo sobre la evolución de ambientes litorales durante el Pleistoceno tardío-Holoceno: Laguna Mar Chiquita (Buenos Aires) - Caleta Valdes (Chubut). In Simposio" Oscilaciones del nivel del mar durante el ultimo hemiciclo deglacial en la Argentina". CONICET, CAPICG, IGCP 61, 27–47.

Figini, A., 1992. Edades 14C de sedimentos marinos holocénicos de la provincia de Buenos Aires. Actas de las Terceras Jornadas Geológicas Bonaerenses 1, 147–151.

Flexor, J.M., Martin, L., 1979. Sur l'utilisation des gres coquilliers de la region de Salvador (Bresil) dans la reconstruction des lignes de rivages Holocenes. In: Proceedings of the 1978 International symposium on coastal evolution in the Quaternary, pp. 343–355.

Fontes, N.A., Moraes, C.A., Cohen, M.C.L., Alves, I.C.C., França, M.C., Pessenda, L.C.R., Francisquini, M.I., Bendassolli, J.A., Macario, K., Mayle, F., 2017. The impacts of the middle holocene high Sea-Level stand and climatic changes on mangroves of the jucuruÇu river, southern Bahia-Northeastern Brazil. Radiocarbon 59, 215–230. https://doi.org/10.1017/RDC.2017.6.

Fucks, E., De Francesco, F.O., 2003. Ingresiones marinas al norte de la ciudad de Buenos Aires. In: Su Ordenamiento Estratigráfico. Actas 2º Congreso Argentino de Cuaternario y Geomorfología, pp. 101–103.

Garrett, E., Melnick, D., Dura, T., Cisternas, M., Ely, L.L., Wesson, R.L., Jara-Munoz, J., Whitehouse, P.L., 2020. Holocene relative sea-level change along the tectonically active Chilean coast. Quat. Sci. Rev. 236, 106281.

Gherardi, D.F.M., Bosence, D.W.J., 2005. Late Holocene reef growth and relative sea-level changes in Atol das Rocas, equatorial South Atlantic. Coral Reefs 24, 264–272. https://doi.org/10.1007/s00338-005-0475-5.

González, M.A., Ravizza, G., 1987. Sedimentos estuáricos del Pleistoceno tardío y Holoceno en la isla Martín García, río de la Plata. Rev. Asoc. Geol. Argent. 42, 231–243.

Gordillo, S., Coronato, A.M.J., Rabassa, J.O., 1993. Late Quaternary Evolution of a Subantarctic Paleofjord. Tierra del fuego, Science Reviews.

Gowan, 2023a. Comparison of the PaleoMIST 1.0 ice sheet margins, ice sheet and paleo-topography reconstruction with paleo sea level indicators (2.0). Zenodo. https://doi.org/10.5281/zenodo.7923553.

Gowan, E.J., 2023b. Paleo Sea-level indicators and proxies from Greenland in the GAPSLIP database and comparison with modelled sea level from the PaleoMIST ice-sheet reconstruction. GEUS Bulletin 53. https://doi.org/10.34194/geusb.v53.8355.

Gowan, E.J., Rovere, A., Ryan, D.D., Richiano, S., Montes, A., Pappalardo, M., Aguirre, M.L., 2021a. Last interglacial (MIS 5e) sea-level proxies in southeastern South America. Earth Syst Sci Data 13, 171–197. https://doi.org/10.5194/essd-13-171-2021.

Gowan, E.J., Zhang, X., Khosravi, S., Rovere, A., Stocchi, P., Hughes, A.L.C., Gyllencreutz, R., Mangerud, J., Svendsen, J., Lohmann, G., 2021b. A new global ice sheet reconstruction for the past 80 000 years. Nat. Commun. 12, 1199.

Guida, N., González, M.A., 1984. Evidencias paleoestuáricas en el Sudeste de Entre Ríos, Su evolución Con Niveles Marinos Relativamente Elevados del Pleistoceno Superior Y Holoceno.

Guilderson, T.P., Burckle, L., Hemming, S., Peltier, W.R., 2000. Late Pleistocene Sea level variations derived from the argentine Shelf. Geochem. Geophys. Geosyst. 1 (12).

Guimarães, J.T.F., Cohen, M.C.L., Pessenda, L.C.R., França, M.C., Smith, C.B., Nogueira, A.C.R., 2012. Mid- and late-Holocene sedimentary process and palaeovegetation changes near the mouth of the Amazon River. Holocene 22, 359–370. https://doi.org/10.1177/0959683611423693.

Hall, G.F., Hill, D.F., Horton, B.P., Engelhart, S.E., Peltier, W.R., 2013. A high-resolution study of tides in the Delaware Bay: past conditions and future scenarios. Geophys. Res. Lett. 40, 338–342. https://doi.org/10.1029/2012GL054675.

Hartt, C.F., 1870. Geology and Physical Geography of Brazil. Fields, Osgood & Co., Boston, 620p.

Heaton, T.J., Köhler, P., Butzin, M., Bard, E., Reimer, R.W., Austin, W.E.N., Bronk Ramsey, C., Grootes, P.M., Hughen, K.A., Kromer, B., Reimer, P.J., Adkins, J., Burke, A., Cook, M.S., Olsen, J., Skinner, L.C., 2020. Marine20 - the Marine Radiocarbon Age Calibration Curve (0-55,000 cal BP). Radiocarbon 62, 779–820. https://doi.org/10.1017/RDC.2020.68.

Hijma, M.P., Engelhart, S.E., Törnqvist, T.E., Horton, B.P., Hu, P., Hill, D.F., 2015. A protocol for a geological sea-level database. In: Handbook of Sea-Level Research. Wiley Blackwell, pp. 536–553. https://doi.org/10.1002/9781118452547.ch34.

Hill, D.F., Griffiths, S.D., Peltier, W.R., Horton, B.P., Törnqvist, T.E., 2011. High-resolution numerical modeling of tides in the western Atlantic, Gulf of Mexico, and Caribbean Sea during the Holocene. J Geophys Res Oceans 116. https://doi.org/10.1029/2010JC006896.

Hogg, A.G., Heaton, T.J., Hua, Q., Palmer, J.G., Turney, C.S., Southon, J., Bayliss, A., Blackwell, P.G., Boswijk, G., Ramsey, C.B., Pearson, C., Petchey, F., Reimer, P., Reimer, R., Wacker, L., 2020. SHCal20 Southern Hemisphere calibration, 0–55,000 years cal BP. Radiocarbon 62 (4), 759–778.

Horton, B.P., Shennan, I., 2009. Compaction of Holocene strata and the implications for relative sea-level change. Geology 37, 1083–1086.

Horton, B.P., Edwards, R.J., Lloyd, J.M., 2000. Implications of a microfossil transfer function in Holocene Sea-level studies. Geol. Soc. Spec. Publ. 166, 41–54.

Horton, B.P., Engelhart, S.E., Hill, D.F., Kemp, A.C., Nikitina, D., Miller, K.G., Peltier, W. R., 2013. Influence of tidal-range change and sediment compaction on Holocene relative sea-level change in New Jersey, USA. J. Quat. Sci. 28, 403–411. https://doi.org/10.1002/jqs.2634.

Horton, B.P., Kopp, R.E., Garner, A.J., Hay, C.C., Khan, N.S., Roy, K., Shaw, T.A., 2018. Annual review of environment and resources mapping sea-level change in time. Space, and Probabil. https://doi.org/10.1146/annurev-environ.

Hu, P., 2010. Developing a Quality-Controlled Postglacial Sea-Level Database for Coastal Louisiana to Assess Conflicting Hypotheses of Gulf Coast Sea-Level Change (MSc Thesis). Tulane University, New Orleans.

Hulton, N., Sugden, D., Payne, A., Clapperton, C., 1994. Glacier modelling and the climate of Patagonia during the last Glacial Maximum. Quat. Res. 42, 1–19.

Isla, F.I., Angulo, R.J., 2016. Tectonic Processes along the South America Coastline Derived from Quaternary Marine Terraces. J. Coast. Res. 32, 840–852. https://doi.org/10.2112/JCOASTRES-D-14-00178.1.

Isla, F.I., Bujalesky, G.G., 2008. Coastal Geology and Morphology of Patagonia and the Fuegian Archipelago. In: Developments in Quaternary Science. https://doi.org/10.1016/S1571-0866(07)10010-5.

Khan, N.S., Ashe, E., Shaw, T.A., Vacchi, M., Walker, J., Peltier, W.R., Kopp, R.E., Horton, B.P., 2015. Holocene Relative Sea-Level changes from Near-, Intermediate-, and Far-Field Locations. Curr. Clim. Chang. Rep. 1, 247–262. https://doi.org/10.1007/s40641-015-0029-z.

Khan, N.S., Ashe, E., Horton, B.P., Dutton, A., Kopp, R.E., Brocard, G., Engelhart, S.E., Hill, D.F., Peltier, W.R., Vane, C.H., Scatena, F.N., 2017. Drivers of Holocene Sea-level change in the Caribbean. Quat. Sci. Rev. https://doi.org/10.1016/j.quascirev.2016.08.032.

Khan, N.S., Horton, B.P., Engelhart, S., Rovere, A., Vacchi, M., Ashe, E.L., Törnqvist, T.E., Dutton, A., Hijma, M.P., Shennan, I., 2019. Inception of a global atlas of sea levels since the last Glacial Maximum. Quat. Sci. Rev. 220, 359–371. https://doi.org/10.1016/j.quascirev.2019.07.016.

Khan, N.S., Ashe, E., Moyer, R.P., Kemp, A.C., Engelhart, S.E., Brain, M.J., Toth, L.T., Chappel, A., Christie, M., Kopp, R.E., Horton, B.P., 2022. Relative Sea-level change in South Florida during the past~ 5000 years. Glob. Planet. Chang. 216, 103902.

Kikuchi, R., Leao, Z., 1997. Rocas (Southwestern Equatorial Atlantic, Brazil): an atoll built primarily by coralline algae. In: Proc 8th Int Coral Reef Sym 1, pp. 731–736.

Laborel, J., 1969. Les peuplements de Madréporaires des côtes tropicales du Brésil. Annales de l'Université d'Abidjan 2.

Laborel, J., 1986. Vermetid gastropods as sea-level indicators. In: Sea-Level Research: A Manual for the Collection and Evaluation of Data. Springer Netherlands, Dordrecht, pp. 281–310.

Leaman, C., Beuzen, T., Goldstein, E.B., 2020. Chrisleaman/py-wave-runup: v0.1.10.

Lorscheid, T., Rovere, A., 2019. The indicative meaning calculator – quantification of paleo sea-level relationships by using global wave and tide datasets. Open Geospatial Data, Software and Standards 4. https://doi.org/10.1186/s40965-019-0069-8.

Lyard, F.H., Allain, D.J., Cancet, M., Carrère, L., Picot, N., 2021. Fes2014 global ocean tide atlas: design and performance. Ocean Sci. 17 (3), 615–649.

Macario, K.D., Alves, E.Q., Oliveira, F.M., Scheel-Ybert, R., Dias, F.F., Lima, G.M., 2023. The variable nature of the coastal 14C marine reservoir effect: a temporal perspective for Rio de Janeiro. Quat. Sci. Adv. 11, 100086.

Martin, L., Suguio, K., 1978. Excursionroute along the coastline between the town of Cananéisa (state of São Paulo) and Guaratiba outlet (state Rio de Janeiro). In: Internarional Symposium on Coastal Evolution, pp. 1–98.

Martin, L., Suguio, K., 1989. Excursion route along the Brazilian coast between Santos (state of São Paulo) and Campos (state of Rio de Janeiro). In: International Symposium on Global changes in South America during the Quaternary, p. 2.

Martin, L., Sugion, K., Flexor, J.M., Bittencourt, A.C.S.P., Vilas-Boas, G.S., 1979. Le quaternaire marin bresilien (littoral pauliste, sud fluminese et bahianais). Serie Geologie 11, 95–124.

Martin, L., Bittencourt, A.C.S.P., Vilas Boas, G.S., 1982. Primeira ocorrência de Corais pleistocênicos na costa Brasileira- Datação Do máximo da Penúltima Transgressão.

Martin, L.K., Suguio, J.M., Flexor, J., Dominguez, M.L., Bittencourt, A.C.S.P., 1996. Quaternary Sea-level history along the central part of the Brazilian Coast. Variations in coastal dynamics and their consequences on coastal plain construction. An.Acad. bras.Ci. 68, 303–354.

Martin, L., Suguio, K., Dominguez, J.M.L., Flexor, J.M., 1997. Geologia do Quaternário Costeiro do Litoral Norte do Rio de Janeiro e do Espirito Santo. CPRM Servico Geologico do Brasil, Belo Horizonte.
Martin, L., Bittencourt, A.C.S.P., Dominguez, J.M.L., Flexor, J.M., Suguio, K., 1998. Oscillations or not oscillations, that is the question: comment on Angulo, RJ and Lessa, GC the Brazilian sea-level curves: a critical review with emphasis on the curves from the Paranagua'and Cananeia regions. Mar. Geol. 150, 179–187.
Martin, L., Dominguez, J.M., Bittencourt, A.C., 2003. Fluctuating Holocene Sea levels in eastern and southeastern Brazil: evidence from multiple fossil and geometric indicators. J. Coast. Res. 101–124.
Martínez, S., Rojas, A., 2013. Relative Sea level during the Holocene in Uruguay. Palaeogeogr. Palaeoclimatol. Palaeoecol. 374, 123–131. https://doi.org/10.1016/j.palaeo.2013.01.010.
Martínez, S.A., Rojas, A., Verde, M., Piñeiro, G., 2006. Molluscan Assemblages from the Marine Holocene of Uruguay: Composition, Geochronology, and Paleoenvironmental Signals Palaeontology and Palaeoenvironments of Continental Invertebrates from Argentina View Project Origin and Evolution of the NW Pacific Cenozoic Sand Dollar Fauna View Project.
Melo, E., Machado, D.M., Lisboa, R.C., Romeu, M.A.R., 2016. Overview of tide, wind and wave conditions along the Brazilian coast for coastal engineering practice. IX PIANCCOPEDEC 9.
Milne, G.A., Mitrovica, J.X., 2008. Searching for eustasy in deglacial sea-level histories. Quat. Sci. Rev. 27 (25–26), 2292–2302.
Milne, G.A., Long, A.J., Bassett, S.E., 2005. Modelling Holocene relative sea-level observations from the Caribbean and South America. Quat. Sci. Rev. 24, 1183–1202. https://doi.org/10.1016/j.quascirev.2004.10.005.
Peltier, W.R., Argus, D.F., Drummond, R., 2015. Space geodesy constrains ICE age terminal deglaciation: the global ICE-6G_C (VM5a) model. J. Geophys. Res. Solid Earth 120, 450–487.
Pirazzoli, P.A., 1991. World Atlas of Holocene Sea-Level Changes, vol. 58. Elsevier (Elsevier Oceanography Series), Amsterdam.
Porter, S.C., Stuiver, M., Heusser, C.J., 1984. Holocene sea-level changes along the strait of magellan and beagle channel, Southernmost South America. Quat 22 (1), 59–67.
Prieto, A.R., Mourelle, D., Peltier, W.R., Drummond, R., Vilanova, I., Ricci, L., 2017. Relative Sea-level changes during the Holocene in the Río de la Plata, Argentina and Uruguay: a review. Quat. Int. 442, 35–49. https://doi.org/10.1016/j.quaint.2016.02.044.
Rabassa, J., Coronato, A., Bujalesky, G., Nica Salemme, M.H., Roig, C., Meglioli, A., Heusser, C., Gordillo, S., Roig, F., Borromei, A., Quattrocchio, M., 2000. Quaternary of Tierra del Fuego, Southernmost South America: an updated review.
Reimer, P.J., Reimer, R.W., 2001. A Marine Reservoir Correction Database and on-Line Interface.
Reimer, P.J., Austin, W.E.N., Bard, E., Bayliss, A., Blackwell, P.G., Bronk Ramsey, C., Butzin, M., Cheng, H., Edwards, R.L., Friedrich, M., Grootes, P.M., Guilderson, T.P., Hajdas, I., Heaton, T.J., Hogg, A.G., Hughen, K.A., Kromer, B., Manning, S.W., Muscheler, R., Palmer, J.G., Pearson, C., Van Der Plicht, J., Reimer, R.W., Richards, D.A., Scott, E.M., Southon, J.R., Turney, C.S.M., Wacker, L., Adolphi, F., Büntgen, U., Capano, M., Fahrni, S.M., Fogtmann-Schulz, A., Friedrich, R., Köhler, P., Kudsk, S., Miyake, F., Olsen, J., Reinig, F., Sakamoto, M., Sookdeo, A., Talamo, S., 2020. The IntCal20 Northern Hemisphere Radiocarbon Age Calibration Curve (0-55 cal kBP). Radiocarbon 62, 725–757. https://doi.org/10.1017/RDC.2020.41.
Ribeiro, S.R., Valadão, R.C., Gomes, M.O.S., Bittencourt, J.S., Alves, R.A., 2023. Paleoecological indicators of the highstand sea level on the Amazonian supralittoral until the last two millennia. J. S. Am. Earth Sci. 104422.
Ribolini, A., Aguirre, M., Baneschi, I., Consoloni, I., Fucks, E., Isola, I., Mazzarini, F., Pappalardo, M., Zanchetta, G., Bini, M., 2011. Holocene beach ridges and coastal evolution in the Cabo Raso bay (Atlantic Patagonian Coast, Argentina). J. Coast. Res. 27, 973–983. https://doi.org/10.2112/JCOASTRES-D-10-00139.1.
Rostami, K., Peltier, W.R., Mangini, A., 2000. Quaternary marine terraces, sea-level changes and uplift history of Patagonia, Argentina: comparisons with predictions of the ICE-4G (VM2) model of the global process of glacial isostatic adjustment. Quat. Sci. Rev. 19, 1496–1525.
Rovere, A., Antonioli, F., Bianchi, C.N., 2015. Fixed biological indicators. In: Handbook of Sea-Level Research, pp. 268–280.
Rovere, A., Raymo, M.E., Vacchi, M., Lorscheid, T., Stocchi, P., Gómez-Pujol, L., Harris, D.L., Casella, E., O'Leary, M.J., Hearty, P.J., 2016. The analysis of last Interglacial (MIS 5e) relative sea-level indicators: Reconstructing Sea-level in a warmer world. Earth Sci. Rev. https://doi.org/10.1016/j.earscirev.2016.06.006.
Rovere, A., Ryan, D.D., Vacchi, M., Dutton, A., Simms, A.R., Murray-Wallace, C.V., 2023. The World Atlas of last Interglacial Shorelines (version 1.0). Earth Syst Sci Data 15, 1–23. https://doi.org/10.5194/essd-15-1-2023.
Rovere, A., Pappalardo, M., Richiano, S., Ryan, D.D., Rubio-Sandoval, K., Ruiz, P.M., Montes, A., Gowan, E.J., 2025. Reconstructing past sea-level changes from storm-built beach ridges. Geomorphology 109659. https://doi.org/10.1016/j.geomorph.2025.109659.
Rubio-Sandoval, K., Ryan, D.D., Richiano, S., Giachetti, L.M., Hollyday, A., Bright, J., Gowan, E., Pappalardo, M., Austermann, J., Kaufman, D., Rovere, A., 2024. Quaternary and Pliocene Sea-level changes at Camarones, Central Patagonia, Argentina. Quat. Sci. Rev. 345, 108999.
Ryan, W.B.F., Carbotte, S.M., Coplan, J.O., O'Hara, S., Melkonian, A., Arko, R., Weissel, R.A., Ferrini, V., Goodwillie, A., Nitsche, F., Bonczkowski, J., Zemsky, R., 2009. Global Multi-Resolution Topography synthesis. Geochem. Geophys. Geosyst. 10 (3).
Santamaria-Aguilar, S., Schuerch, M., Vafeidis, A.T., Carretero, S.C., 2017. Long-term trends and variability of water levels and tides in Buenos Aires and Mar del Plata, Argentina. Front. Mar. Sci. 4, 380.
Schellmann, G., 2007. Bamberger geographische schriften herausgegeben von Heft 22 Teil I: Holozäne Meeresspiegelschwankungen-ESR-Datierungen aragonitischer Muschelschalen-Paläotsunamis. Institut für Gepgraphie an der Universitäat Bamberg, Bamberg.
Schellmann, G., Radtke, U., 2000. ESR Dating Stratigraphically Well-Constrained Marine Terraces Alongthe Patagonian Atlantic Coast (Argentina).
Schellmann, G., Radtke, U., 2003. Coastal Terraces and Holocene Sea-Level changes along the Patagonian Atlantic Coast. J. Coast. Res. 983–996.
Schellmann, G., Radtke, U., 2010. Timing and magnitude of Holocene Sea-level changes along the middle and south Patagonian Atlantic coast derived from beach ridge systems, littoral terraces and valley-mouth terraces. Earth Sci. Rev. 103, 1–30. https://doi.org/10.1016/j.earscirev.2010.06.003.
Shennan, I., 2015. Handbook of sea-level research: Framing research questions. In: Handbook of Sea-Level Research. Wiley Blackwell, pp. 3–25. https://doi.org/10.1002/9781118452547.ch2.
Shennan, I., Tooley, M.J., Davis, M.J., Andrew Haggart, B., 1993. Analysis and interpretation of Holocene Sea-level data. Nature 302.
Shennan, I., Bradley, S.L., Edwards, R., 2018. Relative Sea-level changes and crustal movements in Britain and Ireland since the last Glacial Maximum. Quat. Sci. Rev. 188, 143–159. https://doi.org/10.1016/j.quascirev.2018.03.031.
Smith, C., Salles, T., Concejo, A.V., 2020. pyReefmodel/RADWave: RADWave: Python code for ocean surface wave analysis by satellite radar altimeter.
Souza, M.C., Angulo, R.J., Pessenda, L.C.R., 2001. Evolução geológica e paleogeográfica da planície costeira de Itapoá, litoral norte de Santa Catarina. Revista Brasileira de Geociências 31, 223–230.
Spada, G., Stocchi, P., 2007. SELEN: a Fortran 90 program for solving the "sea-level equation". Comput. Geosci. 33, 538–562.
Stuiver, M., Polach, H.A., 1977. Discussion Reporting of 14 C Data. Radiocarbon 19, 355–363. https://doi.org/10.1017/s0033822200003672.
Stuiver, M., Reimer, P.J., Reimer, R.W., 2021. CALIB Radiocarbon Calibration, Version 8.2. http://calib.org.
Styron, R., 2019. GEMScienceTools/gem-global-active-faults: First release of 2019.
Suguio, K., Martin, L., 1978. Formaçoes Quaternarias Marinhas Do Litoral Paulista e Sul Fluminense = Quaternary Marine Formations of the State of Sao Paulo and Southern Rio de Janeiro.
Suguio, K., Flexor, J.M., Nacional, O., 1980. Le Quaternaire Marin brésilien (Littoral Pauliste, Sud Fluminense et Bahianais).
Sulzbach, R., Klemann, V., Knorr, G., Dobslaw, H., Dümpelmann, H., Lohmann, G., Thomas, M., 2023. Evolution of global ocean tide levels since the last glacial maximum. Paleoceanogr Paleoclimatol 38. https://doi.org/10.1029/2022PA004556.
Tamura, T., 2012. Beach ridges and prograded beach deposits as palaeoenvironment records. Earth Sci. Rev. https://doi.org/10.1016/j.earscirev.2012.06.004.
Toniolo, T., Giannini, P.C.F., Angulo, R.J., de Souza, M.C., Pessenda, L.C.R., Spotorno-Oliveira, P., 2020. Sea-level fall and coastal water cooling during the late Holocene in Southeastern Brazil based on vermetid bioconstructions. Mar. Geol. 428, 106281.
Törnqvist, T.E., González, J.L., Newsom, L.A., van der Borg, K., de Jong, A.F.M., Kurnik, C.W., 2004. Deciphering Holocene Sea-level history on the U.S. Gulf Coast: a high-resolution record from the Mississippi Delta. GSA Bull. 116, 1026–1039. https://doi.org/10.1130/B2525478.1.
Törnqvist, T.E., Rosenheim, B.E., Hu, P., Fernandez, A.B., 2015. Radiocarbon dating and calibration. In: Handbook of Sea-Level Research. Wiley Blackwell, pp. 347–360. https://doi.org/10.1002/9781118452547.ch23.
Tushingham, A.M., Peltier, W.R., 1992. Validation of the ICE-3G Model of Wurm-Wisconsin Deglaciation using a Global Data Base of Relative Sea Level Histories. J. Geophys. Res. Atmos. 97 (B3), 3285–3304. https://doi.org/10.1029/91JB02176.
US Geological Survey, E. H. P, 2017. Advanced National Seismic System (ANSS) comprehensive catalog of earthquake events and products: Various.
Vacchi, M., Engelhart, S.E., Nikitina, D., Ashe, E.L., Peltier, W.R., Roy, K., Kopp, R.E., Horton, B.P., 2018. Postglacial relative sea-level histories along the eastern Canadian coastline. Quat. Sci. Rev. 201, 124e146. https://doi.org/10.1016/j.quascirev.2018.09.043.
van Andel, T.H., Laborel, J., 1964. Recent high relative sea level stand near Recife, Brazil. Science 1979 (145), 580–581. https://doi.org/10.1126/science.145.3632.580.
van de Plassche, O., 1986. Sea-Level Research: A Manual for the Collection and Evaluation of Data. Geo Books, Norwich.
Vos, K., Splinter, K.D., Harley, M.D., Simmons, J.A., Turner, I.L., 2019. Coastsat: a google earth engine-enabled python toolkit to extract shorelines from publicly available satellite imagery. Environ. Model. Softw. 122, 104528.
Vos, K., Harley, M.D., Splinter, K.D., Walker, A., Turner, I.L., 2020. Beach slopes from satellite-derived shorelines. Geophys. Res. Lett. 47 (14) e2020GL088365. e2020GL088365 2020GL088365.
Zanchetta, G., Consoloni, I., Isola, I., Pappalardo, M., Ribolini, A., Aguirre, M., Fucks, E., Baneschi, I., Bini, M., Ragaini, L., Terrasi, F., Boretto, G., 2012. New insights on the Holocene marine transgression in the Bahía Camarones (Chubut, Argentina). Ital. J. Geosci. 131, 19–31. https://doi.org/10.3301/IJG.2011.20.
Zanchetta, G., Bini, M., Isola, I., Pappalardo, M., Ribolini, A., Consoloni, I., Boretto, G., Fucks, E., Ragaini, L., Terrasi, F., 2014. Middle- to late-Holocene relative sea-level changes at Puerto Deseado (Patagonia, Argentina). Holocene 24, 307–317. https://doi.org/10.1177/0959683613518589.